LASER & PHOTONICS REVIEWS

www.lpr-journal.org

Photonic Technologies for Liquid Biopsies: Recent Advances and Open Research Challenges

Francesco Dell'Olio, Judith Su, Thomas Huser, Virginie Sottile, Luis Enrique Cortés-Hernández, and Catherine Alix-Panabières*

The recent development of sophisticated techniques capable of detecting extremely low concentrations of circulating tumor biomarkers in accessible body fluids, such as blood or urine, could contribute to a paradigm shift in cancer diagnosis and treatment. By applying such techniques, clinicians can carry out liquid biopsies, providing information on tumor presence, evolution, and response to therapy. The implementation of biosensing platforms for liquid biopsies is particularly complex because this application domain demands high selectivity/specificity and challenging limit-of-detection (LoD) values. The interest in photonics as an enabling technology for liquid biopsies is growing owing to the well-known advantages of photonic biosensors over competing technologies in terms of compactness, immunity to external disturbance, and ultrahigh spatial resolution. Some encouraging experimental results in the field of photonic devices and systems for liquid biopsy have already been achieved by using fluorescent labels and label-free techniques and by exploiting super-resolution microscopy, surface plasmon resonance, surface-enhanced Raman scattering, and whispering gallery mode resonators. The current state-of-the-art is critically reviewed here, starting from the requirements imposed by the detection of the most common circulating biomarkers. Open research challenges are considered together with competing technologies, and the most promising paths of improvement are discussed for future applications.

1. Introduction

The term "liquid biopsy" was coined for the first time in 2010 and was introduced referring to a new diagnostic concept related to comprehensive and real-time tumor information collection by analyzing circulating tumor cells (CTCs) in the bloodstream.[1] More recently, this term has been broadened to include the analysis of circulating tumor-derived factors, in particular, cell-free tumor DNA (ctDNA), as well as extracellular vesicles (EVs), cell-free microRNAs (cfmiRNAs), mRNA, long non-coding RNA, small RNA, circulating cell-free proteins, and lately, tumor-educated platelets (TEPs).[2] Liquid biopsy is a minimally invasive procedure based on sampling blood, cerebrospinal fluid, urine, sputum, ascites, and theoretically any other body fluid. It is progressively becoming a viable alternative for real-time cancer follow-up in patients and for the assessment of biomarkers that are usually tested only in tissue biopsies.

The analysis of tissue biopsies is currently the gold standard for tumor characterization and treatment decisions. However, there are many limitations to consider: i) tissue biopsies are invasive, ii) some tumor sites are difficult to access with a syringe (e.g., lung or brain), iii) sequential tissue biopsies in individual patients for real-time monitoring of therapy response are difficult or even impossible in clinical practice, iv) a single biopsy at tumor diagnosis can miss minor but relevant tumor clones due to intrapatient tumor heterogeneity, and v) the procedure can be time-consuming.[3] Conversely, liquid biopsy offers significant advantages, including i) it is a noninvasive procedure, ii) it is easily repeatable, iii) a quick turn-around of

Dr. F. Dell'Olio
Department of Electrical and Information Engineering
Polytechnic University of Bari
Bari 70125, Italy
E-mail: francesco.dellolio@poliba.it
Prof. J. Su
Department of Biomedical Engineering, College of Optical Sciences, and BIO5 Institute
University of Arizona
Tucson, AZ 85721, USA

The ORCID identification number(s) for the author(s) of this article can be found under https://doi.org/10.1002/lpor.202000255

DOI: 10.1002/lpor.202000255

Prof. T. Huser
Biomolecular Photonics, Department of Physics
University of Bielefeld
Bielefeld 33615, Germany
Prof. V. Sottile
Department of Molecular Medicine
University of Pavia
Pavia 27100, Italy
Prof. V. Sottile
School of Medicine
University of Nottingham
Nottingham NG7 2RD, UK
Dr. L. E. Cortés-Hernández, Dr. C. Alix-Panabières
Laboratory of Rare Human Circulating Cells (LCCRH)
University Medical Center of Montpellier
Montpellier 34093 CEDEX 5, France

results can be provided, iv) the procedure is feasible in all patients regardless of the location of the primary tumor or distant metastases, v) the procedure offers a way to detect aggressive clones disseminating from different sites (primary tumors and/or metastatic sites), vi) it is compatible with real-time monitoring of disease progression and drug response, and vii) it provides the ability to identify resistance mechanisms to different drugs over the course of treatment. However, liquid biopsy should not be seen as a substitute for histopathological diagnoses, due to the clinical importance of other morphological features that are impossible to assess without tissue. Nevertheless, the analysis of liquid biopsy in cancer represents the natural extension of the metastatic cascade. Indeed, liquid and tissue biopsies are complementary and of primary importance for the analysis of the whole cancer progression. Thus, by using both approaches, it is possible to get a holistic evaluation of cancer, which can be used as part of an innovative cancer management strategy.[3]

Liquid biopsies are bioanalytical procedures whose development and validation require multidisciplinary contributions from a range of experts with a wide range of backgrounds, i.e., physicians, biologists, biochemists, biophysicists, and engineers. The workflow for each liquid biopsy analysis consists of a sequence of several steps that depend on the specific biomarker under study. The process starts with the body fluid collection phase; then, the sample is properly processed (e.g., by fixation, immunofluorescent staining, magnetic bead isolation, and ultracentrifugation) following standardized operating procedures to make it suitable for the successive key steps, that is, quantitative biomarker detection and, eventually, further molecular characterization.

Several well-established bioanalytical techniques with relevant instrumentation readily available on the market, such as immunocytochemical analyses and nucleic acid-based technologies, are currently used to perform detection and characterization steps for liquid biopsies. These methods and instruments often use photonics. In particular, the physical phenomenon of fluorescence excitation or imaging and microscopy systems with different configurations are bulky, time-consuming, expensive, and require highly skilled operators to obtain reliable results. Aiming at developing point-of-care tools for liquid biopsy with short response times (on the order of minutes), microphotonics, nanophotonics, and nanoplasmonics are emerging as key enabling technologies due to the typical advantages of photonic biosensing technology, i.e., compactness, high-resolution, low cost, immunity to noise and external disturbance, and compatibility with CMOS electronics technology. In addition to the scientific interest toward photonic micro/nanotechnologies, the field of photonics for liquid biopsy is also exploring the use of new fluorescence-based nanoscopy techniques to enhance the performance of conventional imaging systems. These can typically aid in the investigation of the spatial distribution of receptors on the cell surface, their quantitation, and the characterization of their interactions with ligands.

In this paper, recent advances in the field of photonic technologies for liquid biopsy are reviewed with a specific emphasis on current and future applications in oncology and ensuing requirements. The photonic technologies presented here, which typically have a medium (from 3 to 5) technology readiness level (TRL), will be compared both to well-established technologies, including those that have already reached the commercialization stage, and to emerging technologies that are not photonics-based.

2. Circulating Tumor Biomarkers

As mentioned above, liquid biopsies include not only CTCs, but also new promising circulating biomarkers released by tumor cells. This section describes their biogenesis, biology, and preanalytical and bioanalytical steps to detect them in the bloodstream of cancer patients. Some selected high-TRL methodologies and technologies already on the market for implementing these steps are mentioned, and their biological and bioanalytical aspects are highlighted. Finally, the clinical perspectives of liquid biopsies are discussed. All these aspects are summarized in **Figure 1**.

2.1. Circulating Tumor Cells

Research on CTCs is a very active field; more than 25 574 publications were listed under the keywords "circulating tumor cell" in PubMed by June 2020 (on average, 40 new publications were added each week in 2020). CTCs represent the ideal biosource for solid cancer characterization and monitoring as they i) are released actively by primary tumor and/or metastatic sites and ii) can be characterized at different levels (genome, proteome, transcriptome, and secretome). CTCs are rare in the bloodstream; however, recent high-technology methods allow the enrichment, detection, isolation, and characterization of single CTCs.[1,2]

During the last decade, significant progress has been made in the development of different technologies to study CTCs as well as in the discovery and validation of new CTC markers. To identify the right CTC markers, the biology of CTCs and normal immune cells needs to be considered. The "ideal" CTC marker would be expressed on all CTCs but not on the surrounding leukocytes and would never be downregulated during dissemination. As CTCs are rare (1–5/7.5 mL of blood), they are first concentrated (several log units) before being detected.

Enrichment methods rely on biological properties (e.g., surface protein expression) and physical properties (e.g., size, density, electric charge, and deformability). The first strategy based on biology could be divided into two subgroups of technologies: positive selection where CTCs are captured directly based on the expression of surface markers, e.g., epithelial cell adhesion molecules, (EpCAM) or negative selection when normal surrounding blood cells are depleted based on the expression of known surface markers, e.g., cluster of differentiation 45, CD45. Among the current positive selection systems, the CellSearch system is the only technology cleared by the US Food and Drug Administration (FDA) available on the market. By being robust and reproducible, this technology has shown the clinical validity and utility of CTCs in metastatic breast cancer diagnosis.[4,5] Interestingly, capturing CTCs that are negative or with a very low expression of EpCAM have stimulated the use of antibodies directed against various other epithelial cell surface antigens (e.g., epidermal growth factor receptor (EGFR) epithelial mucin 1 or against tissue-specific antigen (e.g., prostate-specific antigen (PSA); human epidermal growth factor receptor 2, HER2) and against mesenchymal or stem-cell antigens (e.g., snail; aldehyde

Figure 1. Circulating biomarkers as liquid biopsy for precision medicine. In a blood sample, different complementary circulating biomarkers can be detected, isolated, and characterized. This figure summarizes the bioanalytical techniques of tumor-educated platelets, circulating tumor cells, circulating cell-free tumor DNA, extracellular vesicles (e.g., exosomes) and cell-free RNA (e.g., i) noncoding RNA with miRNA, snRNA & snoRNA and lncRNA, and ii) messenger RNA), cell-free proteins as well as their clinical relevance. Abbreviations: TEP, tumor educated platelet; CTC, circulating tumor cell; ctDNA, circulating tumor DNA; cfRNA, cell-free RNA; cfmiRNA, cell-free microRNA; snRNA, small nuclear RNA; lncRNA, long noncoding RNA; mRNA, messenger RNA; RNA-Seq, RNA sequencing; EpCAM, epithelial cell adhesion molecule; CK, cytokeratin; RT-qPCR, reverse-transcription-quantitative polymerase chain reaction; EGFR, epithelial growth factor receptor; KRAS, V-Ki-ras2 Kirsten rat sarcoma viral oncogene homolog; AR, androgen receptor; PIK3CA, phosphatidylinositol-4,5-bisphosphate 3-kinase catalytic subunit alpha; ESR1, estrogen receptor 1; ALK, anaplastic lymphoma kinase; PD-L1, programmed death-ligand 1; HER2, human epidermal growth factor receptor-2; HR, hormone receptor; AR-V7, androgen receptor splice variant 7; PSMA, prostate-specific membrane antigen; Safe-Seqs, safe-sequencing system; CAPP-Seq, cancer personalized profiling by deep sequencing; TAM-Seq, tagged-amplicon deep sequencing; CNA, copy number aberrations; WGS, whole genome sequencing; WES, whole exome sequencing.

dehydrogenase 1).[6] The second strategy is based on the physical properties of CTCs: most of them generally exhibit a larger morphology and are stiffer than leukocytes; thus, they can be concentrated by using technologies based on their size and deformability, e.g., filtration membranes and microfluidic chips.

After the enrichment step, the sample is rarely pure with just CTCs remaining; leukocytes are still present, and CTCs need to be specifically identified at the single-cell level. For this purpose, immunological technologies are the most frequently used methods for CTC detection using a combination of membrane and/or intracytoplasmic antiepithelial, antimesenchymal, and antitissue specific markers or antitumor-associated antibodies. Nucleic acid-based methods can represent alternatives to immunological assays, but their low specificity could lead to false positive results.[3] Another CTC identification approach focuses on detecting proteins secreted, released, or shed from viable cancer cells cultured for 24–48 h. This unique functional assay is called epithelial immunospot (EPISPOT).[7] A completely new microdroplet technology to detect viable CTCs at the single-cell level called EPIDROP is currently being optimized.[2] The limit of CTC detection depends entirely on the methodology and technology used for sample preparation, enrichment, and enumeration. For example, the CellSearch system can detect only 1 CTC per 7.5 mL of blood, and specific cutoffs have been defined to provide clinically relevant data in localized and metastatic cancer patients.

In the final step, CTCs can be characterized at different levels: genome, epigenome, transcriptome, proteome, secretome, and function.[8] Indeed, by analyzing the genome of CTCs, specific mutations can be identified to drive therapy.[2] For instance, detecting the spliced variant 7 of the androgen receptor in prostatic CTCs can predict resistance to endocrine therapy.[9,10] The expression of the protein death ligand 1, an immune checkpoint regulator and therapeutic target, could be detected on CTCs and may help drive immunotherapy.[11] Finally, the functional analysis of CTCs is of utmost importance for understanding the biology of the metastatic cascade. Thus, the in vitro or in vivo expansion of CTCs could identify the metastasis-competent CTCs that are the most aggressive subset of CTCs at the origin of the metastatic relapses in cancer patients.[2,12]

2.2. Circulating Tumor DNA

CtDNA is DNA found in the bloodstream (or any biological fluid) and is released mainly by dying cancer cells.[2,13,14] CtDNA research is quite recent compared to that of CTCs, with around 5485 publications listed under the keywords "circulating tumor DNA" in PubMed by June 2020. As most circulating cell-free DNA (cfDNA) comes from normal cells under physiological conditions, ctDNA represents only a small fraction (<0.01%) of cfDNA. This biological material is highly fragmented DNA, mainly derived from apoptotic cells, predominantly from apoptotic leukocytes.

During the early stages of cancer in patients without distant metastases, the concentration of ctDNA is very low, and many groups have used different strategies to detect ctDNA in plasma samples from cancer patients. In that case, the analysis of the primary tumor is needed to identify a single tumor-specific mutation or a panel of mutations before detecting ctDNA in the bloodstream. First, targeted DNA sequencing techniques such as digital polymerase chain reaction (dPCR), bead–emulsion–amplification–magnetics (BEAMing) technology, the safe-sequencing system (Safe-SeqS), cancer personalized profiling by deep sequencing (CAPP-Seq), and tagged-amplicon deep sequencing (TAmSeq) need to be mentioned. These methods are more sensitive than nontargeted sequencing approaches, with ctDNA detection limits of <0.01%; however, they first require the characterization of the primary tumor. Second, nontargeted next-generation sequencing (NGS) is used for genome-wide analysis of copy number aberrations, point mutations, and/or other genetic aberrations by whole-genome sequencing (WGS) or whole-exome sequencing (WES). The advantage of this approach is the detection of mutations in minor clones present in the primary lesion or metastatic sites that can then be selected during adjuvant therapy or during the natural postoperative progression of the disease. However, a real problem of genome-wide ctDNA analyses compared to targeted approaches is the need for higher concentrations of ctDNA and lower overall assay sensitivity (above 1–5%), which limits their utility in patients without metastatic disease before disease relapse.[2] Four years ago, two new methods were proposed: a mass spectrometry-based approach (UltraSEEK) and an assay combining surface-enhanced Raman spectroscopy and PCR.[15,16] Being fairly new technologies, they still require further validation; however, they have the potential to achieve analyses with low amounts of DNA, while maintaining high sensitivity and specificity. Finally, epigenetics has an important role in cancer. Thus, researchers put considerable effort on the analysis of ctDNA methylation; it can be assessed by methylation-specific PCR, which requires large amounts of ctDNA.[3,17]

2.3. Extracellular Vesicles

EVs include exosomes, microvesicles, microparticles, oncosomes, apoptotic bodies, lipoprotein particles, and any other nonviral vesicle secreted or shed from cells. Exosomes, which are membrane vesicles of endocytic origin (30–150 nm diameter) and with a density between 1.15 and 1.19 g mL^{-1} are the most studied EVs.[18–20] Exosome research shows that around 5398 publications were listed under the keywords "tumor exosomes" in PubMed by June 2020. They are involved in many different physiological and pathological processes such as intercellular communication, proliferation, cell migration, cancer metastasis, and immunomodulatory activities. Exosomes secreted from a malignant cell often reflect the molecular composition of the cell of origin.[21] This aspect was described in early studies in the field, and Johnstone et al. already in 1987 identified that exosomes from reticulocytes have a similar phospholipid composition than the cells of origin.[22] The loading of molecules into the exosomes is a selective process that is not yet completely clarified.[23] Exosomes are stable carriers of enriched genetic material and proteins from their cells of origin, thereby holding great promise as biomarker for identifying early stage tumors. This analyte is systematically detectable in the blood, urine, saliva, and other biological fluids of patients with different cancer types. Interestingly, the release of exosomes from tumor cells is an active process with concentrations $\geq 10^9$ vesicles mL^{-1}

in blood. So far, it is challenging to differentiate tumoral from nontumoral exosomes (or EVs) in blood; however, it has been shown that cancer patients yield higher numbers of EVs and their enumeration or characterization could theoretically predict the progression of the disease.[24] Still, the clinical evaluation of EVs or exosomes in a patient aims to improve the minimally invasive detection of biomarkers, which could be possible even when the purity of the isolation methods is not perfect. Anyway, current methods should be seen more as enrichment methods with a bias for specific subtypes of EVs, and with different levels of purity and yields. Additionally, different EVs might have different clinical meanings and applications.[25,26]

The gold standard method for EV isolation is ultracentrifugation, which consists of multiple centrifugation steps (of >100 000 g) of samples containing EVs.[27] Density gradient ultracentrifugation (isopycnic and rate-zonal centrifugation) uses a density gradient inside the ultracentrifugation tube to trap specific EVs according to their density (e.g., exosomes).[27] Under these conditions, EVs can be enriched with the highest purity, but with a low yield; however, the procedure is time-consuming and requires the use of ultracentrifugation equipment. Alternative procedures are based on size (size exclusion chromatography) and ultrafiltration, or immunomagnetic beads against EV surface markers (e.g., tetraspanins).[3,28,29] For instance, size exclusion chromatography is based on columns of Sepharose with specific porosity, that in case of EVs, can theoretically separate vesicles and particles of the size of exosomes. Even though this method is simple, isolated EVs are usually diluted and it is difficult to operate for large volumes. Alternatively, immunomagnetic beads-based methods can offer a better approach to select subpopulations of EVs and can be used as commercial kit easily; however, the lack of understanding of EVs heterogeneity hampers the utility of this approach. Moreover, surface markers of exosomes are shared among different vesicles, which makes it technically difficult to isolate this kind of vesicles using a single marker.[30] These methods are promising as a higher EV yield can be obtained, and most of them could be easily introduced into clinical departments as there is no need for specialized equipment. Nevertheless, these methods often have high heterogeneous yields of EVs.[25] More recently, microfluidic microchips and acoustic waves have also been proposed to isolate pure EVs.[31]

Exosomes have been shown to correlate with tumor progression, immune response suppression, angiogenesis, and metastasis.[32] The nucleic acid cargo of EVs and exosomes can be used to detect biomarkers with demonstrated clinical utility, such as the mutations of EGFR; the isolation of EVs with this purpose can theoretically improve the enrichment of these nucleic acids and provide better quality than those used for circulating-free DNA or RNA.[33] Exosomes show specific miRNA related with their biological function, which could offer new biomarkers in cancer, for instance: miR-100, miR21, mir155, miR1246, just to mention some examples.[34–37] Moreover, nucleic acids might be protected from degradation and being in the exosomes increases their quality and "half-life" in blood. Still, due to the lack of standardization in methods, it is difficult to establish if current methods for circulating-free DNA or RNA are in fact detecting the nucleic acids inside EVs or vice versa. Furthermore, some authors have shown that nucleic acids, specially DNA, might not be part of the exosomal cargo, or that other vesicles such as large EVs (oncosomes) bodies hold most of the DNA.[14–38] As more robust methods appear, these issues will be clarified in a near future. Finally, the potential of exosomes is huge, not only for their use as biomarkers, but also because these EVs can be used as carry-on particles to deliver therapeutic molecules to specific tissues and sites.

2.4. Cell-Free RNAs

While DNA content is mostly identical in different cells of an organism, transcriptional profiles can vary dramatically across cell types, space, and time. Therefore, changes in the transcriptome offer an opportunity to associate cellular phenotypes to underlying molecular mechanisms and potential genotypic changes. Consequently, RNA is an excellent candidate. Indeed, RNA detection presents higher sensitivity and specificity compared with protein biomarkers and its analysis is less expensive. Moreover, compared with DNA, RNA biomarkers provide better dynamic insights into cell regulation and states. With the advent of RNA-Seq, transcriptomics has arguably become a mature omics approach in the functional genomics toolset.[39]

2.4.1. Noncoding RNAs

There are a large variety of noncoding RNA species that could be used as cancer biomarkers in liquid biopsies. Among them, the most studied are microRNAs, but recently the attention of researchers has also been directed toward Piwi-interacting RNAs, circular RNAs, and other small noncoding RNAs.[23] Another class of RNA species, the long noncoding RNAs, is larger than microRNAs and represents a very versatile and promising group of molecules which, apart from their use as biomarkers, also have a possible therapeutic role.

Cell-Free miRNA: miRNA research shows around 670 publications listed under the keywords "cell-free miRNA" in PubMed by June 2020. miRNAs are fragments of single-stranded noncoding RNA (ncRNA) of 19–25 nucleotides, derived from hairpin precursor molecules that comprise 70–120 nucleotides. Expression patterns of miRNAs are unique to individual tissues and differ between cancer and normal tissues.[40] They act predominantly as translational repressors by binding to complementary sequences in the 3′untranslated region of their target mRNAs. However, there is growing evidence indicating that miRNAs can also serve as activators of gene expression by targeting gene regulatory sequences. Many miRNAs have been reported to be dysregulated and involved in several types of cancers, which makes sense when considering their general action as either oncogenes or tumor suppressors. Most cfmiRNAs bind with AGO2 (protein of the Argonaute family), whereas a minority of specific cfmiRNAs are predominantly associated with vesicles.[41] In contrast to long molecules of RNA species (i.e., mRNA), circulating miRNAs are highly stable: they are resistant to degradation at room temperature for up to 4 days and in deleterious conditions such as boiling, are stable after multiple freeze–thaw cycles, and insensitive to high or low pH.[42]

The detection methods for cfmiRNAs are essentially the same as that for cellular miRNAs: northern blotting, in situ

hybridization, reverse transcriptase-PCR (RT-PCR), microarray, and deep sequencing. However, the extremely low initial amount of starting material in the liquid biopsy needs to be considered; thus, preanalysis factors need to be considered (e.g., sample preparation and RNA extraction methods). The three major techniques for detecting cfmiRNA are i) quantitative RT-PCR (the gold standard to quantify cfmiRNAs and cellular miRNAs, the stem-loop primer method, and the polyA-tailed PCR); ii) microarrays (high-throughput format for genome-wide comprehensive profiling of all miRNAs in various types of samples including body fluids); iii) deep sequencing (miRNA-seq, profiling all expressed miRNAs). Concerning the clinical relevance of cfmiRNA, numerous studies have reported cfmiRNAs as diagnostic and prognostic markers for different cancer types. Moreover, their signatures are reported to be related to tumor development, disease progression, and metastases.[2,43]

More recently, it has been shown that, besides miRNA, other ncRNAs, such as ultraconserved genes, could expand the spectrum of ncRNA biomarkers (long ncRNAs, circular RNAs, small RNA).[44]

SnRNAs and SnoRNAs: Small nuclear (snRNA) and small nucleolar (snoRNA) RNAs are components of the small ncRNAs transcriptome. Both are 60- to 300-nucleotide long and transcribed from intronic sequences of coding genes.[23]

snRNAs are located in the cell nucleus and are fundamental in RNA–RNA remodeling, in spliceosome assembly, being implicated in the translation process.[45] Alterations in snRNA structure have been reported, and their functional consequences could be implied in the oncogenic process.[46] The best-known snRNA released into body fluids is U2: it has been detected in serum or plasma of lung, colorectal, pancreatic, and ovarian cancers.[23]

snoRNAs are hosted in introns of coding and noncoding transcripts and are implicated in the posttranscriptional modification of rRNA.[23] In 2019, two snoRNAs (snoRA74A and snoRA25) detected in serum exosomes resulted as good biomarkers, able to distinguish pancreatic cancer patients from controls.[47]

LncRNAs: LncRNAs constitute a heterogeneous group of noncoding transcripts of >200 nucleotides that may be distributed in various cellular compartments. They can be intragenic (intronic or antisense) or intergenic.[23] The biological functions of lncRNAs are various: from coordinating gene regulation at DNA/RNA level to regulation of protein biogenesis and function. They play an important role in carcinogenesis and metastasis, and they seem to be key players in cancer biology, considering them as potential cancer diagnostic and prognostic factors.[23,48]

2.4.2. mRNAs

Aberrant mRNA expression levels are associated with dysregulation in cancer. Comprehensive profiling of gene expression patterns across many tissues and cancers have yielded molecular classifications of cancer (sub)types.[49] Furthermore, unbiased sequencing of transcripts has enabled detection of cancer- and patient-specific somatic mutations and fusions/rearrangements, spearheading the discovery of novel mRNA biomarkers.[50] Shen et al. reported that plasma mRNA as liquid biopsy predicts chemo-sensitivity in advanced gastric cancer patients.[51] More recently, Chang et al. observed that transcriptomic analysis in liquid biopsy identifies circulating PCTAIRE-1 mRNA as a biomarker in nonsmall cell lung cancer (NSCLC).[52]

2.5. Circulating Cell-Free Proteins

Proteomic analyses have opened a new avenue for cancer biomarker discovery and several multi-marker tests are currently available on the market.[53,54] This subsection summarizes some examples of cell-free proteins used in blood- or urine-based tests, also called tumor markers, already commercially available or in development.

2.5.1. Breast Cancer—Blood Test

Although multiple serum-based tumor markers have been described for breast cancer, such as CA 15-3, BR 27.29 (CA27.29), carcinoembryonic antigen (CEA), tissue polypeptide antigen, tissue polypeptide specific antigen, and HER-2 (the extracellular domain); still the most widely used are CA 15-3 and CEA.[55] CA 15-3 is one of the first circulating prognostic factors for breast cancer. Preoperative concentrations thus might be combined with existing prognostic factors for predicting outcome in patients with newly diagnosed breast cancer. At present, the most important clinical application of CA 15-3 is in monitoring therapy in patients with metastatic breast cancer that is not assessable by existing clinical or radiological procedures.[54]

2.5.2. Prostate Cancer—Blood Test

The PSA is a protein produced by both normal and cancer cells; in the prostate gland PSA is mostly found in semen, but a small amount can also be found in the serum. No biomarker has affected the clinical management of cancer more than PSA.[56] The risk of having prostate cancer goes up as the PSA level goes up, however this maker is not cancer-specific. The usual cut-off is 4 ng mL^{-1} or higher when a man might need further testing. PSA has also been proposed as an early detection screening marker. For this purpose, an ultrasensitive immunoassay has been developed: The single molecule assay (SIMOA, Quanterix Corp). This assay has shown, in an in vivo model, to archive significantly higher sensitivity for the detection of PSA than the standard ELISA assays. However, further validation of this method is still needed.[57]

The prostate health index (PHI) is a blood-based test that provides a probability of prostate cancer (PCa) by combining three tests (PSA, free PSA, and p2PSA) into a single score.[58] The higher specificity of PHI means a greater probability of identifying those patients who actually need a biopsy, allowing for a substantial decrease in the current number of prostate biopsies being ordered and reported as negative for cancer. According to a metaanalysis of eight studies, comprising 2969 men, PHI is superior to measuring free PSA alone for prostate cancer detection at first biopsy in men with total PSA values of 2–10 ng mL^{-1}.[59]

The 4KScore is a blood test for assessing the risk of aggressive prostate cancer. This multi-marker blood test combines the results of total PSA, free PSA, intact PSA, and human kallikrein 2 (hK2) for assessment of significant (Gleason>7) prostate cancer before biopsy.[60]

2.5.3. Immunotherapy—Blood Test

The major limitations of immune checkpoint inhibitors (such as pembrolizumab) are i) high cost, ii) limited success rate and potential severe toxicity due to immune-related adverse events. Predictive biomarkers that can predict the likelihood of a cancer patient responding favorably to therapy or developing toxicity are urgently needed to overcome these limitations.[61] The authors reported that highly multiplexed assays for measuring thousands of serum proteins simultaneously may have utility in identifying these biomarkers.

2.5.4. Melanoma—Blood Test

Rucevic performed proteomic profiling of patient plasma samples to build a predictor of immunotherapy response and uncover biological insights underlying primary resistance.[62] The authors worked on an initial cohort comprising 55 metastatic melanoma patients receiving anti-PD1 (Pembrolizumab or Nivolumab) and subsequently on 116 patients as a validation cohort. They could report a panel of proteins as biomarkers that can predict responses to the immunotherapy and elucidate resistance to cancer immunotherapy in patients with metastatic melanoma.[62]

2.5.5. Nonsmall-Cell Lung Cancer—Blood Test

Sheng et al. reported that heat shock protein 27 (HSP27) is related to tumorigenesis.[63] Moreover, they showed that increased HSP27 expression correlated with shorter survival of NSCLC patients ($p < 0.001$), suggesting that HSP27 may serve as a potential biomarker for diagnosis and prognosis of NSCLC.

2.5.6. Thyroid Cancer—Blood Test

The improvement in the accuracy of targeted proteomic assays such as the multiple reaction monitoring (MRM), has opened the opportunity to detect thyroglobulin in serum of patients with thyroid cancer. MRM is used instead of immune-assays, due to the high abundance of auto-antibodies in this set of patients, which affects the detection rate, giving up to 25% of false negative results; the MRM method is not affected by this issue. Moreover, although thyroglobulin is found at extremely low level, MRM still provides high sensitivity to detect the protein.[64,65]

2.5.7. Bladder Cancer—Urine Test

The Aura Tek FDP TestTM is a urine-based test that measures fibrin degradation products (FDPs) for the detection of bladder cancer recurrence.[66] The test is intended to be used on voided urine specimens in conjunction with cytologic analysis and increases overall sensitivity for all grades of tumor while maintaining the high specificity of conventional cytology.

ImmunoCyt/uCyt+ is an immunocytochemical urine-based test developed by Fradet and Lockhard in 1997.[67] It detects three markers that are commonly found on malignant exfoliated urothelial cells: cytoplasmic mucins and high-molecular-weight form of glycosylated CEA for urothelial carcinoma diagnosis.[68]

2.5.8. Limitations of Circulating Cell-Free Proteins as Tumor Markers

Even though proteomic and immunoassays offer an opportunity to multiplex the detection of different protein markers, other methods based on nucleic acids are technically less challenging and in many cases are more affordable. So far, the economic cost might be the major limitation, as these methods might require high affinity antibodies (i.e., ELISA or MRM) and/or specialized equipment that is not easily accessible by all clinical laboratories. Moreover, protein markers might be very unspecific and lack sensitivity to detect cancer when they are not used in the correct clinical context, which could lead to confusing results and subsequently unnecessary interventions. It might even increase the health-associated cost and risk to the patients.

Despite some remaining challenges, proteomic-based research shows clinical promise to introduce even more proteins in the liquid biopsy. In addition, the improved sensitivity, specificity, and the clinical success of multi-marker assays have driven the shift from a single- to multi-marker view. It could be easily achieved based on the scalability of both target proteomic and immunoassay methods.

2.6. Tumor-Educated Platelets

The new area of TEPs research shows only 50 publications listed under the keywords "tumor-educated platelets" in PubMed by June 2020.

Platelets are anucleated cell fragments that originate from megakaryocytes. They are key players in hemostasis, thrombosis, immunity, inflammation, and metastasis.[3,69–76] Gasic et al. showed that tumors can induce platelet aggregation and correlated this with metastases in a mouse model. The authors suggested that activated and aggregated platelets interact with tumor cells and increase tumor cell extravasation to the metastatic niche.[77] Although platelets are easy to purify, it is crucial to prevent their activation during experiments because it highly affects their molecular and morphological characteristics; consequently, strong mechanical or biochemical forces should be avoided.[78–80] Blood should be gently collected using a 1.2 mm intravenous cannula and TEPs can be isolated up to 48 h after blood sampling, allowing the isolation of high-quality RNA for molecular tests.[81–83] By performing messenger RNA (mRNA) sequencing of TEPs, Best et al. could distinguish 228 patients with localized and metastatic tumors from 55 healthy individuals with 96% accuracy. In addition, based on TEP mutational status, they could obtain key information to predict the tumor type. Thus, TEPs are shown to be involved as central players in systemic and local responses to tumor growth.[84] In conclusion, even blood platelets could also provide a valuable platform for pan-cancer, multiclass cancer, and companion diagnostics, possibly enabling clinical advances in blood-based liquid biopsies.[85]

2.7. Clinical Perspectives of Liquid Biopsies

Cancer research is increasingly focusing on early detection and is using precision medicine for the stratification of patients, prediction of treatment efficacy, identification of metastatic

relapse, mechanisms of drug resistance, and therapeutic targets. Real-time liquid biopsy will play a crucial role in these processes (Figure 1). It is important to mention that CTCs, ctDNAs, EVs, cell-free RNAs, circulating cell-free proteins, and TEPs are complementary circulating biomarkers and may be combined based on the cancer type, as in some multianalyte tests under development (e.g., Freemone that considers three classes of biomarkers, cfDNA, cfRNA, and protein from blood, and CancerSEEK detecting solid tumors by combining ctDNA and protein biomarkers), and be introduced in clinical practice in the near future.[86,87] An algorithm should be developed to combine all these data to obtain a more precise tumor profile.[88] In particular, machine learning algorithms for big data processing are currently used in the context of liquid biopsies because they have the unique feature of reducing large numbers of measurements into lower-dimensional outputs.[89] For example, an automated machine learning platform to analyze liquid biopsy data has been recently reported.[90] It was specifically designed for liquid biopsy data and has the very interesting capability to continuously improve itself as the quantity of the processed liquid biopsy data increases.

Very recently, the feasibility of blood testing combined with a full-body diagnostic positron emission tomography-computed tomography has been reported to screen for cancer and guide intervention.[91]

Liquid biopsy analysis has provided new insights into the biology of metastasis, with important implications for the clinical management of cancer patients. Numerous clinical studies and metaanalyses including large cohorts of patients have shown that the number of CTCs is an important indicator of the risk of progression or death in patients with metastatic and localized solid cancer (e.g., breast, prostate, and colon).[92] Moreover, longitudinal ctDNA analyses have provided interesting insights into the dynamics of tumor evolution.[93] The clinical relevance of EVs as a single biomarker has not yet been established. However, EVs can provide important information for cancer prognosis and diagnosis, mostly in combination with other circulating biomarkers, such as CTCs.[94] Finally, TEPs may be used as a minimally invasive biomarker for cancer detection and progression monitoring.[83,85]

An interesting example of ctDNA-based liquid biopsy is the Cobas EGFR Mutation Test v2. It is a real-time PCR test that identifies 42 mutations in exons 18, 19, 20, and 21 of the EGFR gene, including the T790M resistant mutation, by analyzing ctDNA from plasma samples of nonsmall cell lung cancer patients. It is designed to enable testing of both tissue and plasma specimen with a single kit and has a specificity and sensitivity of 99.8% and 65.7%, respectively.[95] It has been approved by the FDA and the European Medicines Agency with the specific recommendation that plasma cfDNA analysis should be performed first to avoid unnecessary invasive biopsies of the lung (with subsequent tumor biopsy analysis if no EGFR mutation is detected in cfDNA).[96]

It is important to highlight that CTC measurements have shown their clinical validity for many years; however, they have not yet been included in the clinical guidelines because their clinical utility is still under investigation.[4] Thus, interventional studies on treatment stratification based on the analysis of CTCs (enumeration and/or characterization) and ctDNA are urgently needed to implement liquid biopsy into personalized medicine with reimbursement for cancer patients.[97] The validation of liquid biopsy assays and their introduction into clinical practice is an important task that will be the main focus of the new European Liquid Biopsy Society (ELBS) comprising more than 60 institutions from academia and industry.[98]

3. Imaging Platforms Based on High-Speed and High-Resolution Fluorescence Microscopy

Imaging cytometry at high speed and high spatial resolution has become a recent topic of rapidly growing interest in the field of liquid biopsy. While commercially available flow cytometers can currently operate at up to 40 different color channels and obtain information from millions of cells in a matter of seconds, the resulting multi-dimensional data sets are still difficult to analyze and require considerable human interaction and experience. This type of single cell analysis can also be performed in vivo in animal models, for example, by multi-photon excited fluorescence microscopy, permitting the identification and visualization of leukocytes for instance, or even that of circulating stem cells and their interaction with local tissues.[99–103] While being widely used in diagnostics and research, pure flow measurements cannot typically take advantage of additional morphological parameters of interest, such as the distribution of organelles, vesicles, or even receptors throughout the cell and their dynamic behavior, all of which require fast imaging of cells with subwavelength spatial resolution. Recently, a number of highly advanced optical microscopy techniques have emerged that can, however, provide this information. Quantitative phase microscopy is one of the fastest and most sample-friendly imaging techniques, which, especially when combined with instant multiplane imaging, provides high-resolution 3D morphological maps of single living cells.[104–106] Another exciting development is the ultrafast imaging of cells in flow using a process called serial time-encoded amplified microscopy (STEAM) and its more recent variants.[107,108] This method takes advantage of the broad spectral bandwidth and the high repetition rate of modern ultrashort lasers, in particular fiber lasers. While this technique enables the extremely fast morphological characterization of cells, there is, however, also a need for higher specificity and sensitivity, which until now has mostly required fluorescent labels.

Many super-resolving fluorescence microscopies, which achieve a spatial resolution well beyond the optical diffraction limit, can now address this need. Historically, this trend started with our ability to detect single fluorescent molecules and, with another, more physical technique, taking advantage of shaping the illumination and detection point spread functions of optical microscopes.[109–111] Indeed, the detection of a single fluorescent molecule by an optical imaging system with the highest possible optical resolution that high-end objective lenses can provide, still limits the resulting image of a molecule to a spot size with physical dimensions of approximately half the wavelength, that is, typically ≈250 nm in diameter. This resulting "spot" is typically referred to as the point spread function of the optical system. Single fluorescent molecules can be distinguished only if they are separated by more than approximately the width of the point spread function, unless other parameters, such as different fluorescent colors, are used

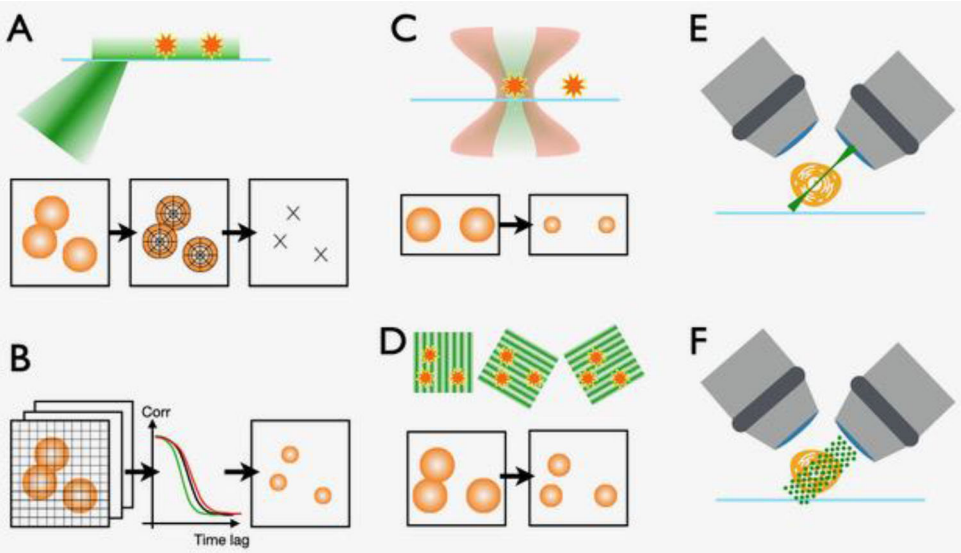

Figure 2. Schematic descriptions of several advanced forms of high-resolution microscopy. A) PALM/STORM microscopy: fluorophores are excited by a laser beam hitting the cover glass surface near or beyond (shown here) the angle of total internal reflection. The resulting spots in the fluorescence image can be attributed to single fluorescent molecules that are localized with ≈10 nm accuracy. B) SOFI: fluctuating signals from molecules are pixel-wise correlated and cross-correlated, resulting in a higher-resolution image. C) STED: a tightly focused excitation beam is superposed with a shaped de-excitation beam, resulting in higher resolution images by raster-scanning of the beams. D) SIM: an interference pattern is rotated and shifted across the sample. Analysis in Fourier space allows for 2× higher image resolution by advanced mathematical reconstruction algorithms. E) Bessel-beam microscopy: a highly focused, elongated excitation beam is swept across the sample, resulting in an extremely thin light sheet. Fluorescence is collected by a second microscopy objective lens held at 90° with respect to the beam. F) Lattice-light sheet microscopy: multiple elongated beams interfere with each other resulting in a lattice-like excitation pattern.

to determine their location independently from each other.[112] Indeed, once a spot has been identified as the image of a single molecule, its location, that is, the centroid of the resulting spot, can be determined with very high precision.[113] Thus, the ability to actively influence (switch) the fluorescence behavior of single molecules by using photoactivatable localization microscopy (PALM), or by analyzing their stochastic intermittent fluorescence emission with stochastic optical reconstruction microscopy, (STORM), can be used to determine if a single molecule has indeed been identified, and could thus enable the detection of cancer biomarkers in patient biopsy material.[114,115] By collecting typically thousands of images, where the location of single molecules is determined down to ≈20 nm, images with a spatial resolution on the scale of a few 10 s of nanometers can then be constructed, as shown in **Figure 2**A.[113,114] Similarly, at higher labeling densities, the analysis of the temporal emission behavior of fluorescent molecules can be utilized to obtain images with increased spatial resolution in a process named super-resolution optical fluctuation imaging (Figure 2B).[116] Parallel to this development, engineering the illumination point spread function, for example, by overlaying a diffraction-limited excitation spot with a high-power donut-shaped de-excitation spot by depleting the excited state of fluorescent molecules in a process named stimulated emission depletion (STED), laser-scanning fluorescence microscopy images can readily be obtained at a spatial resolution that can be tuned based on the efficiency of the depletion process, with ≈80 nm spatial resolution being the most typical choice (Figure 2C).[111] By exploiting the engineering of the illumination point spread function to the scale of the entire field of view, that is, by inducing interference patterns onto the sample (in a process most widely known as structured illumination microscopy, SIM), fluorescence images with approximately twice the spatial resolution can be obtained in three dimensions, as shown in Figure 2D.[117–119] A particular problem of most of these methods is, however, their dependence on high illumination powers, which has detrimental effects on the biological samples under investigation. While SIM, with its typically more modest resolution improvement, has been demonstrated to work well for high-speed imaging of fluorescently labeled cells, a number of derivatives of these techniques have also recently been developed. Among them are Bessel beam light sheet and lattice light sheet microscopy, see Figure 2E,F, which provide illumination modes similar to SIM, but can penetrate deeper into the sample, and which can readily be combined with single-molecule localization methods to provide highest-resolution 3D images.[120–122]

Super-resolution-based approaches thus offer notable resolution, with low sample requirements and fast analytical protocols that are particularly appealing for the study of small targets, such as single biomarkers and extracellular vesicles, extracted from cancer cell cultures or liquid biopsies for analysis.[123,124] Hence, many of the techniques mentioned above have already been successfully applied to liquid biopsy.

Super-resolution microscopy was recently used to detect, localize, and quantify the expression of CD13 in cancer cells through 3D molecular imaging (3DMI).[125] This technique, based on the use of a fluorescently tagged anti-CD13 antibody and the 3D reconstruction of SIM images, enabled the fine quantification of the cancer biomarker on the membrane of single leukemic cells. This approach confirmed cell-to-cell variability in the level of

surface expression, which correlated with cell sensitivity to a specific inhibitor molecule applied in vitro. This 3DMI study underlines the potential benefits of a precision medicine approach, whereby a fine analysis of specific molecular features on patient cells may inform the potential outcome of a given therapeutic approach. Similarly, dSTORM single-molecule detection revealed the presence of ultralow expression levels of surface oncoantigens that remained undetected in myeloma cells using standard cytometric methods.[126] dSTORM was successfully used to screen patient cells, and elucidated the correlation between the presence of these ultralow markers and cancer sensitivity to immunotherapeutic intervention, suggesting a wider applicability for additional cancer types. The growing range of RNA signatures associated to specific cancer types, such as breast and cervical or glioblastoma for instance, provides a set of possible targets in the form of microRNAs and lncRNAs amenable to affinity-based tagging for fluorescence imaging.[127–129] Furthermore, a recently described protein-based detection approach applicable to accelerate single-molecule super-resolution imaging of nucleic acids could facilitate the use of this technology to the survey of specific cancer RNA biomarkers in patient samples for therapeutic management.[130] Dual molecule imaging performed with PALM/STORM has also been applied to refine the characterization of cell-derived exosomes, and to provide phenotypic information, such as the co-expression of CD63 and HER2 on the surface of breast cancer-derived exosomes.[124] Intracellular distribution and trafficking of these cancer-derived vesicular components could likewise be monitored postinternalization into normal cells, highlighting the cross-talk between cancer-derived exosomes and other cell populations.

STED microscopy was used to determine the redistribution of the viral envelope glycoprotein in single virus particles of HIV-1 following viral maturation.[131,132] This achievement should eventually enable the dynamic visualization of the maturation process and its importance during virus transmission from infected to uninfected T cells. Using STED and SIM, Eggeling and co-workers were able to visualize the spatial organization and importance of actin in the formation of immunological synapses in resting and activated T cells. By employing high spatial resolution and high speed, low phototoxic imaging modalities of SIM and lattice light sheet microscopy, they were recently able to follow the rearrangement of this cytoskeletal protein in living T cells.[133,134] Although single molecule localization microscopy methods require substantially longer image accumulation times to acquire the number of images needed to reconstruct high-resolution maps of protein distributions by exploiting total internal reflection illumination combined with SOFI, Lukeš et al. were able to determine the distribution of CD4 glycoprotein mutants on the nanoscale in the plasma membrane of T cells.[135] Similarly, to avoid any contact with substrates, which, even when coated with polymers that block adherent cells, can adversely affect T cells, Diekmann et al. developed a combination of optical tweezers and single molecule localization microscopy.[136,137] Here, single cells are first captured by highly focused laser beams in the near-infrared (1064 nm). The laser beams are reflected by a spatial light modulator placed in the Fourier plane of the setup, which allows the researchers to dynamically create and control optical traps in a process called holographic optical tweezers. By holding onto single cells and capturing ≈30 000 individual

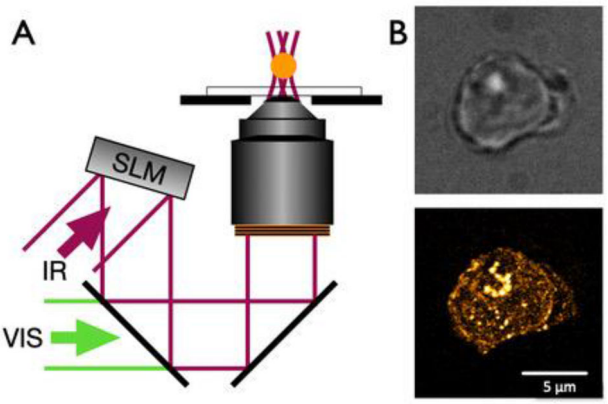

Figure 3. Localization microscopy in combination with holographic optical tweezers (HOT). A) Schematics of a combined localization microscopy and HOT setup, where a spatial light modulator (SLM) is used to create multiple optical traps with a near-infrared (IR) laser beam to immobilize nonadherent cells, such as T cells. Excitation of fluorescently labeled samples is achieved, e.g., by STORM-like excitation with a visible (VIS) laser beam. B) White-light transmitted (upper image) and STORM image (lower image) of single trapped T cells infected with the human immunodeficiency virus (HIV-1), which is labeled by immunofluorescence.

images of fluorescent molecules in these cells, Diekmann et al. reconstructed images with 100 nm spatial resolution utilizing a deconvolution approach that compensated for residual sample motion within the optical traps. **Figure 3**A schematically shows how a single cell captured by holographic optical tweezers is visualized by STORM, and Figure 3B shows an example of the outcome of such an experiment with an optically trapped T cell. Another exciting development along similar lines is the approach using planar waveguide chips as substrates through which single fluorescent molecules are excited.[138] Once such chips can be manufactured in high volume, they will enable an inexpensive and widely accessible implementation of super-resolution microscopy on existing microscope setups, which could facilitate the analysis of circulating tumor cells in clinical environments. The separation of excitation and detection optics also supports a much broader choice of detection objective lenses, thereby increasing the field of view at the expense of slightly reduced spatial resolution. In the field of high-speed volumetric imaging of living cells at high spatial resolution, lattice light sheet microscopy of white blood cells is particularly noteworthy.[139] This method enabled Cai et al. to dynamically follow the formation of an immunological synapse between a T cell and an antigen-presenting cell and to determine that microvilli, i.e., protrusions on the surface of T cells, are actively involved in the antigen recognition process and change their dynamics upon recognition.

This short survey serves to provide an initial outline of possibilities opened up by super-resolution optical microscopies. Another exciting and currently very promising area of research along these lines is the recent combination of spatially structured illumination methods and single-molecule localization. By exploiting well-characterized illumination patterns, such as the inside of a donut spot or sinusoidal patterns of structured illumination microscopes, even higher-resolution images can be acquired with minimal photon doses. This was very impressively and convincingly demonstrated by Balzarotti et al. using the donut

pattern, and recently extended to SIM-like patterns independently by four research groups.[140–144] These methods offer exciting prospects for true molecular-level 3D resolution in cells.[145]

Currently, employing advanced optical microscopy techniques to conduct liquid biopsy is still cumbersome at multiple levels, starting with the special requirements placed on sample preparation. In the majority of cases, sample preparation typically requires the fixation of cells obtained either from cell cultures or from patients because both the staining techniques as well as the image acquisition process are not yet compatible with live cell imaging. Background autofluorescence, light scattering, the quality of the fluorescent labels, and the quality of the labeling process itself all play crucial roles in the ultimate success of obtaining high-quality super-resolved images from single cells. Another problem particularly relevant to liquid biopsy is the fact that blood-borne cells do not spontaneously adhere to substrates, or, if they do, they can become activated or change behavior in other ways compared to that available when imaging them in their native environment. Acquiring high-quality images from these samples also requires highly skilled operators to understand the optical system as well as the biological relevance of the samples, and the same is true for the analysis of the resulting data. While the automation of some of these processes is emerging, for example by developing "smart microscopes" that can autonomously obtain raw data over long periods of time, or by utilizing deep learning procedures for image reconstruction and analysis, the full integration of these methods into a single system is still a challenge.[146]

4. Sensing Platforms Based on Plasmon Resonance and Surface-Enhanced Raman Scattering

Plasmonics is widely used in the field of molecular biology and biomedicine to study several aspects of biospecific interactions without using fluorescent labels. Its enabling role in the field of liquid biopsies is discussed in this section with a focus on the recent advances based on surface plasmon resonance (SPR), localized surface plasmon resonance (LSPR), and surface-enhanced Raman scattering (SERS).

4.1. Surface Plasmon Resonance

SPR is the resonant coupling between surface plasmons, that is, collective oscillations in the electron density at the surface of a metal, and monochromatic polarized light.[147] This coupling usually takes place at a metal/dielectric planar interface when the wave vectors of TM-polarized light and surface plasmons are matched through the Kretschmann setup, where a focused light beam is directed toward a glass prism, on which a thin metal layer is deposited, and is reflected by the metal/dielectric interface.[148]

SPR, which is one of the most mature label-free analytical techniques, is widely used in life sciences to study biochemical phenomena involving a functionalization biolayer immobilized on the metal layer and target biomolecules or their assemblies dispersed in a solution, and occurs at nanometer distance, typically 150–200 nm, from the dielectric/metal interface.[149] The interaction between the functionalization layer and the analyte induces a change in the thickness and/or refractive index of the biolayer on the metal film and, in turn, of the resonance condition characterizing the SPR. Because the intensity of light reflected by the metal layer is minimal when the resonance condition is fulfilled, the analyte concentration can be estimated by monitoring the resonance angle through a properly arranged photodiode array.

Gold is by far the preferred metal in the field of SPR sensors for life sciences because its functionalization via thiol chemistry is quite easy, it is relatively inert, and allows SPR excitation through visible or near-infrared light, whose sources are typically low cost.[150]

The SPR-based sensing concept can be expanded to implement an SPR imaging (SPRi) platform, where the metal layer is properly functionalized by robotic spotters depositing nanoliter droplets of ligand solutions on the surface according to a 2D predefined pattern of hundreds of spots with a diameter of 200–500 μm.[151,152] Light incident on the thin metal film is reflected with different intensities by the spots according to the biochemical reactions taking place there. By using a charge-coupled device camera to detect the reflected light, hundreds of biochemical reactions can be simultaneously analyzed, according to a very efficient multiplexed approach.

SPR instruments have been on the market since 1990, when the first Biacore instrument was commercially released, and there have been many experiments in their use in the context of liquid biopsies in the last few years, mainly to detect exosomes and miRNAs.[153]

Exosomes, owing to their diameter ranging from 30 to 100 nm, are well-suited for SPR-based detection, which can only be used for nanometer-sized biomolecules or their assemblies because of their sensitivity to biochemical reactions occurring at a distance of up to a few hundred nanometers from the metal layer.

Rupert et al. reported one of the first attempts to quantitatively detect cancer-derived exosomes using an SPR instrument on the market (Biacore 2000 with an excitation wavelength equal to 760 nm).[154] The target biomolecule assemblies studied were human mast cell-secreted exosomes carrying the tetraspanin membrane protein CD63. By using a quite standard functionalization strategy, based on anti-CD63 antibodies, exosome concentration is estimated by a quantification method that, as for many exosome SPR biosensors, relies on diffusion-limited binding kinetics on the sensor surface. The developed method has a relatively low accuracy in the order of ± 50%. This is due to two key aspects: i) CD63-positive exosomes represent a subpopulation with a diffusion coefficient and size significantly different from the mean diffusion coefficient and size of the whole population of EVs and ii) CD63-positive exosomes are deformed after binding to the surface. To improve the accuracy of their method, the same authors proposed and experimentally studied the use of an SPR instrument on the market (SPR Navi 220A) including two excitation light sources at 670 and 785 nm instead of a standard SPR instrument.[155] With this approach, an improvement of the accuracy down to ± 10% is reported because the particle size on the surface is estimated by the ratio of the instrument responses at the two operating wavelengths.

By using a custom wavelength-modulated SPR platform, a time-consuming analytical method for profiling clinically relevant exosomes has been demonstrated.[156] The platform includes, in addition to a standard prism, a halogen polychromatic

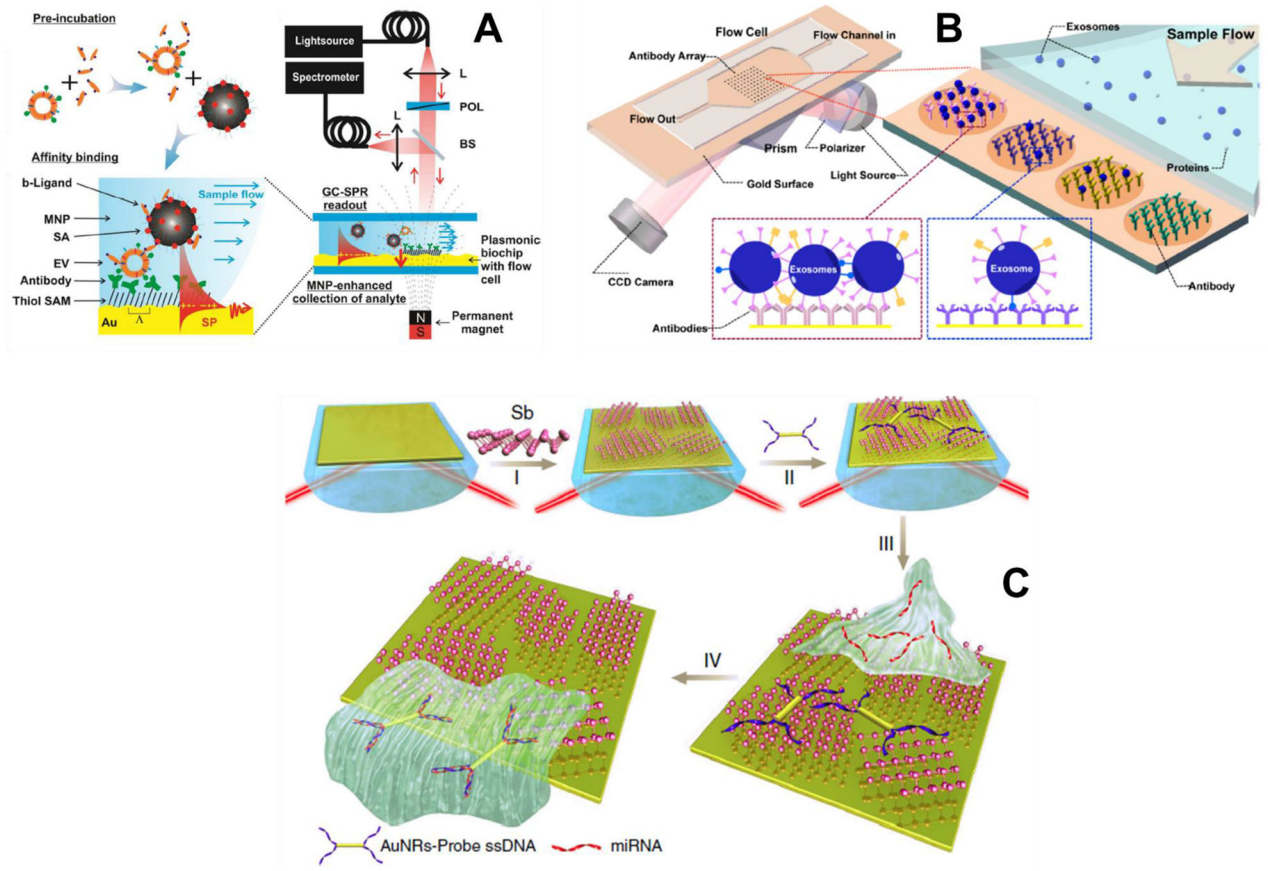

Figure 4. SPR and SPRi platforms for liquid biopsy. A) Magnetic nanoparticle-enhanced grating-coupled (GC) SPR sensor for EVs quantitative detection with the schematic illustration of EVs preincubation with the biotinylated lipid-binding ligand (b-ligand) and streptavidin (SA) coated magnetic nanoparticles (MNPs). SAM: thiol self-assembled monolayer, L: lens, POL: polarizer, BS: beam splitter. Reproduced with permission.[158] Copyright 2017, Royal Society of Chemistry. B) SPRi platform for capturing and detecting exosomes in cell culture supernatant. Reproduced with permission.[160] Copyright 2014, American Chemical Society. C) Antimonene-based SPR sensor for miRNA detection with details on the operating principle and fabrication process including antimonene nanosheet assembly on the Au film I), Gold nanorod-ssDNAs adsorption on antimonene nanosheets II), sensor interaction with miRNA solution III), and release of the gold nanorod-ssDNA from the antimonene nanosheets. Reproduced with permission.[166] Copyright 2019, Springer Nature.

light source (wavelength range: 360–2400 nm) that excites the SPR and a spectrometer for resonance condition monitoring. It allows, in combination with a properly engineered sandwich assay, the estimation of the proportion of tumor-derived exosomes within the bulk exosome population. The same SPR platform in which the gold layer is functionalized by biotinylated anti-HER2 antibodies has been used to detect BT474 breast cancer cell-derived exosomes in complex biological samples with a LoD of 8280 exosomes per µL.[157]

Reiner et al. reported an interesting advancement of SPR biosensors intended for the analysis of EVs, including exosomes.[158] The sensor system, which is a wavelength-modulated grating-coupled SPR platform, is shown in **Figure 4**A. It includes a top-illuminated chip where a relief sinusoidal grating (modulation depth of ≈60 nm and pitch = 430 nm) is manufactured on the surface of the gold film, a broadband halogen light source for SPR excitation, and a spectrometer for analyzing the light beam reflected by the gold layer. The assay concept is based on the use of streptavidin-coated magnetic nanoparticles (NPs) with a diameter of 220 nm that bind to EVs via lipid-binding proteins. This allows an increase in the concentration of the target EVs at the sensor surface by applying a magnetic field gradient generated by a permanent magnet at a distance of 5 mm from the sensor surface. The experimental results demonstrate that the grating-coupled SPR device can detect EVs secreted by mesenchymal stem cells at concentrations down to 0.76 µg mL^{-1}.

To further enhance the LoD of SPR biosensors detecting cancer-derived exosomes, NP-assisted signal amplification has recently been used with an SPR aptasensor, that is, a sensor based on oligonucleotides, also called "chemical antibodies," to bind specific markers on the surface of target exosomes.[159] In this study, functionalized gold NPs (AuNPs) were engineered to detect and quantify EV components. The first aptamer-coated AuNP was used to detect a specific EV membrane marker. Then, the aptamer-coated AuNP was coupled with a second AuNP with nucleotide-based affinity to the first aptamer-AuNP. With this approach, an LoD improvement of 20% is obtained. In this system, the detection of MCF-7 (breast cancer cell line)-derived exosomes were brought down to 5000 mLcells^{-1} mL^{-1} through a selective and reproducible process lasting ≈2.5 h.

Through its multiplexing capability, SPRi, combined with antibody microarray technology, allows direct exosome quantification in tumor cell culture medium, without purification.[160] The system demonstrating this achievement is based on a SPRi instrument on the market (PlexArray HT) where a laser-generated collimated light at 660 nm is directed toward the coupling prism at a fixed angle position, reflected by the SPR active gold surface, and detected by the charge-coupled device (CCD) camera (see Figure 4B). Exosome quantification is obtained by printing and immobilizing antibodies specific to exosome transmembrane proteins on the gold-coated glass sensor chip. In this way, after sample injection into the flow cell, exosomes can be captured by antibodies on the chip. Capture events induce an increase in the average thickness of the biolayer on the gold surface and a change in the refractive index of the same layer. Consequently, in each sensing site (spot) where capture takes place, a change in the reflection intensity is detected by the CCD camera. The same SPRi-based sensing concept has been recently used to develop a biosensing assay for the highly sensitive and multiplex characterization of exosomes from nonsmall cell lung cancer, with an LoD of 10 000 exosomes per µL.[161] This LoD value was achieved by enhancing the assay using antibody-functionalized AuNPs.

In addition to tumor-derived exosomes, SPR and SPRi platforms have demonstrated very good performance in the field of circulating miRNA cancer biomarker detection, with an LoD down to 10×10^{-18} M. The first interesting results of miRNA detection by SPR phenomenon were reported in 2006, when an NP-amplified SPRi approach for miRNA detection with an LoD of 10×10^{-15} M was discussed.[162] After this pioneering paper, several strategies have been developed for sensitivity enhancement in SPR biosensors aimed at circulating miRNA detection. The most used assays are those based on Au or Ag NPs for SPR enhancement, hybridization chain reaction, and DNA-RNA-antibody.[162–165] Xue et al. reported an innovative SPR sensing platform based on antimonene for label-free detection of miRNA-21 and miRNA-155, which are usually overexpressed in several hematological and solid tumors.[166] The antimonene-modified SPR chips used in this platform are shown in Figure 4C. Antimonene nanosheets, having a 2D nanostructure, are assembled on a gold chip surface by a layer-by-layer technique, and gold nanorods that are bioconjugated with single-stranded DNA probes are absorbed on the nanosheets to amplify the SPR signal. After the chip preparation, complementary and noncomplementary miRNA molecules dispersed in phosphate-buffered saline (PBS) solution were injected onto the sensing surface, and the SPR signal was recorded using a commercially available time-resolved SPR spectrometer. The interaction between the target miRNA and the gold nanorod single-stranded DNA complex induces the release of the complex from antimonene, with a consequent significant decrease in the SPR angle. The record LoD equal to 10×10^{-18} M achieved on the platform is attributed by the authors to a combination of two effects: i) a strong interaction between antimonene and single-stranded DNA/double-stranded DNA in terms of the work function change of antimonene due to the interaction with nucleobases and base pairs and ii) the above-mentioned SPR signal amplification due to nanorods.

In addition to the most investigated applications of SPR technology in the field of liquid biopsies, that is, exosomes and miRNA quantitative detection, some papers suggest that SPR and SPRi can also be used to detect single nucleotide polymorphisms, analyze ctDNA methylation, and measure the concentration of protein biomarkers. In particular, NP-enhanced SPRi in combination with DNA microarray technology have been used for point mutation identification in a gene (BRCA1) that is associated with breast cancer, with an LoD equal to 1×10^{-12} M.[167] More recently, Carrascosa et al. reported a label-free and real-time biosensing strategy to detect DNA methylation in a breast cancer cell line (MCF-7).[168] Several nanoparticle-enhanced SPR methods have also been reported for the detection of various proteins cancer biomarkers, including the ErbB2 receptor tyrosine kinase 2 in human serum and raw cancer lysates (LoD = 180 pg mL^{-1}).[169]

4.2. Localized Surface Plasmon Resonance

LSPR is excited when a light beam interacts with metal NPs or metallic nanostructures with dimensions comparable to or smaller than the wavelength of the excitation radiation. Nonpropagating oscillations of free electrons in the conduction band of the metal are generated owing to the interaction.

LSPR usually occurs on the surface of NPs suspended in solution or deposited onto a solid support, or in chip-scale nanofabricated metallic structures, for example, periodic arrays of nanoholes or nanopillars.

Each LSPR phenomenon is associated with a specific plasmon resonance frequency depending on the physical/geometrical features of the NP/nanostructure and suffers from a shift due to any change in the immediate dielectric environment in close proximity to the NP/nanostructure (optimal sensing distance in the order of a few tens of nanometers).

In LSPR-based biosensing platforms, NPs/nanostructures are functionalized with antibodies, nucleic acid strands, and other types of ligands before quantitative detection, which is carried out by evaluating the shift (typically a red shift) in the plasmon resonance frequency caused by the selective capture of the target circulating biomarker by the ligand molecules.

In the context of liquid biopsies, the most interesting LSPR-based platforms that researchers have used for experiments are those based on nanohole/nanopillar arrays intended for the quantitative detection of nanoEVs and those using properly functionalized AuNPs for the sensitive detection of miRNA and ctDNA.

4.2.1. Nanohole/Nanopillar Arrays

One of the most promising LSPR-based approaches for exosome detection is based on the nanoplasmonic exosome (nPLEX) chip, where a 2D periodic lattice (periodicity = 450 nm) of nanoholes with a diameter of 200 nm is patterned in a gold film with a thickness of 200 nm using focused ion-beam milling (**Figure 5**).[170] The chip includes 36 sensing units, each consisting of a lattice of 44 × 32 nanoholes. The sample flowed toward the sensing units through 12 microfluidic channels, each encompassing three measurement sites. By measuring optical transmission through an array that is top-illuminated and label-free, a high-throughput quantitative analysis of exosomes derived from ovarian cancer cells (average diameter of 100 nm)

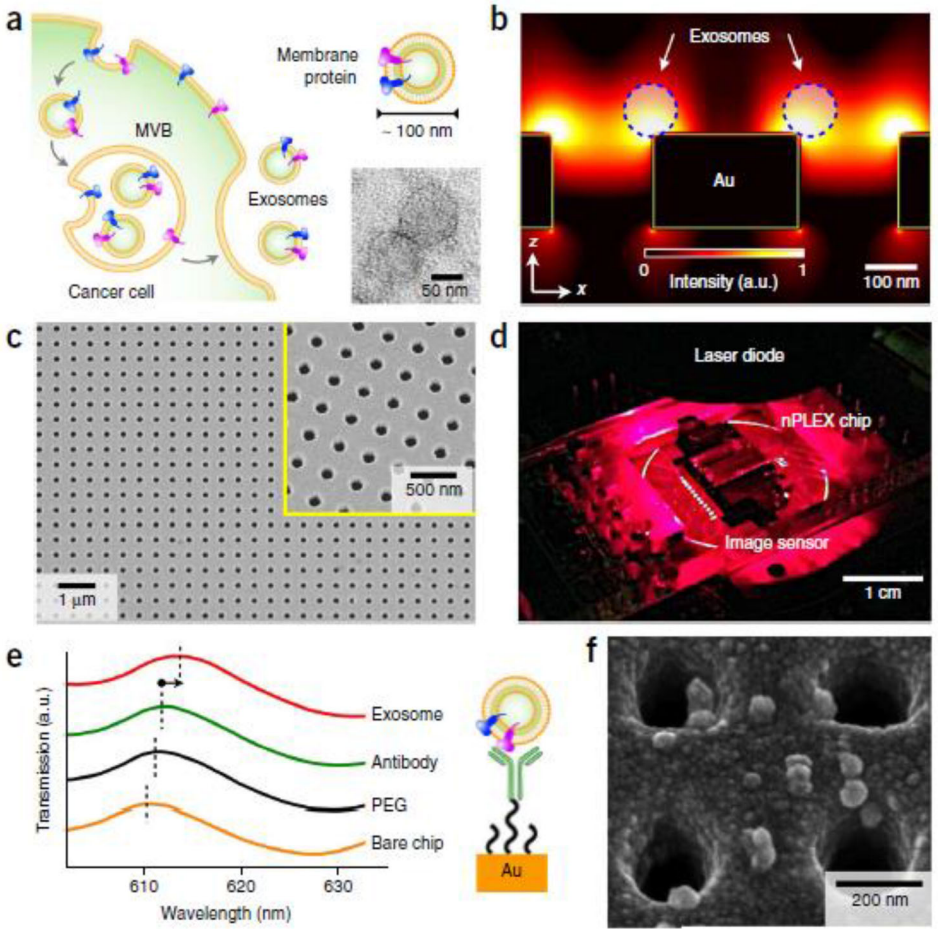

Figure 5. nPLEX chip for label-free exosomes detection with details on exosomes biogenesis involving multivesicular body, MVB a), electromagnetic field distribution close to the nanoholes b), nanoholes array imaged by scanning electron microscopy c), measurement setup d), spectral shift due to functionalization and interaction with exosomes, surface-adsorbed exosomes e). Reproduced with permission.[170] Copyright 2014, Springer Nature.

was demonstrated with an LoD of 3000 exosomes (670×10^{-18} M). The optical interrogation of the sensing unit array is based on a spectral shift of the transmission spectrum or an intensity change measured at the plasmon resonance frequency. It can be carried out either by a standard microscope-based setup including a spectrometer to analyze light transmitted through nPLEX or a portable setup, which includes a laser source at 638 nm, collimating lens, and a square pattern diffuser for the chip illumination, and a CMOS imager measuring the intensity of light transmitted through the chip. The chip functionalization strategy consists of a polyethylene glycol precoating step with a 1:3 mixture of long and short polymer chains minimizing non-specific exosome binding and grafting monoclonal antibodies against cancer protein targets, for example, EpCAM, CD24, and CD41, onto the long polyethylene glycol precoating chains for specific exosome capture. In this way, the authors demonstrate the parallel detection of 12 potential exosomal markers in less than 30 min. In addition, the reported experiments suggest that secondary labeling further enhances the spectral shift in the transmission spectrum, allowing for exosome detection. The enhancement was 20% with spherical Au NPs (diameter, 10 nm) and 300% with star-shaped Au NPs (diameter, 50 nm).

Several sensing platforms that are conceptually similar to the nPLEX platform intended for the quantitative detection of cancer-derived exosomes released by different cancer cell lines have been reported in the literature.[171,172] Zhu et al. reported a more complex LSPR-based periodic nanostructure for exosome detection consisting of a quasi-3D plasmonic photonic crystal, which was designed to confine and enhance the electromagnetic field through hybrid coupling of plasmonic and photonic crystal modes.[173]

A sensing system that is not aimed at characterizing the size and concentration of exosomes but is designed for single exosome detection has been recently reported in the literature.[174] The LSPR imaging platform is based on quartz chips with a diameter of 25.4 mm and includes 20 × 20 arrays of quartz nanopillars (total height ≈490 nm, diameter ≈90 nm, pitch 500 or 600 nm) with 80 nm gold caps on the top. The quantitative detection of exosomes secreted by breast adenocarcinoma cells (MCF7) has been carried out by functionalizing the nanosensors with anti-CD63 antibodies, loading the chips into a microfluidic assembly, and placing it on an inverted microscope. The CMOS camera included in the system is capable of imaging 16 chips and consequently 6400 nanopillars.

4.2.2. Gold NPs

A central limitation for the translational application of SPR technologies to liquid biopsy in cancer resides in the low concentration of circulating oncogenic biomarkers. Hence, the development of ancillary techniques to enhance sensitivity can deliver significant progress toward clinical feasibility.[175] In particular, AuNPs have been successfully combined with synthetic oligonucleotides used as probes to achieve signal amplification through different experimental strategies.

One such approach developed to enhance the LSPR signal using AuNPs involves semiconductor quantum dots (QDs) for a photoinduction-based fluorimetric assay to detect target miRNAs.[176] The detection comes from the binding of the target miRNA with a corresponding synthetic DNA probe, which causes aggregation of the QDs and affects the colorimetric change occurring from the photoinduced AuNP dissolution process at 560 nm. This method, benefiting from a low reagent cost and an estimated LoD of 4.4×10^{-12} M, has been successfully used for the detection of miR-155 present in MCF7 breast cancer cell lysates, although in this model, the concentration could be expected to be significantly above that present in the circulation in cancer patients.

Another strategy to potentiate LSPR detection of low abundancy miRNAs has recently proposed the use of a duplex-specific nuclease (DSN)-mediated step to amplify the initial signal.[177] In this approach, the presence of target miRNA in solution is detected by its hybridization to synthetic DNA probes immobilized onto a gold substrate. The formation of the probe-target hybrid triggers its specific cleavage by the DSN enzyme, releasing the probe in solution as well as the miRNA target itself, which is then available for de novo hybridization to release from another immobilized probe molecule, resulting in specific accumulation of target-specific probes in solution. These miRNA-specific DNA probes released by the DSN-based selection were then quantified using a DNA sandwich-based process, following hybridization chain reaction onto a DNA-functionalized detection chip and adsorption of tannic acid-capped AuNPs acting as nanotags. The key features of this technique are the high specificity of its DSN-mediated step, directly affected by potential base-pair mismatches, and its sensitivity with a calculated LoD of 2.45×10^{-12} M. This technique has demonstrated its efficacy for the detection of cancer-associated miRNA-10b, both in vitro, and in plasma and urine samples isolated from a xenograft mouse model.

Wei et al. reported an alternative signal amplification step for enhanced LSPR detection of specific miRNAs, involving the exponential amplification reaction (EXPAR) of the initial probe recognition event.[178] In this case, initial hybridization of the target miRNA to a complementary probe decorating AuNPs enables the EXPAR amplification step, producing target-specific DNA intermediates that accumulate in suspension. These DNA intermediates, once recognized and bound by a second type of nucleotide-decorated AuNPs, are able to recruit further AuNPs based on the formation of triplex DNA hybrids, thus mediating particle aggregation, which produces a colorimetric read-out. This assay applied to detect miRNA-21 was reported to achieve miRNA selectivity and offer an LoD of 0.23×10^{-15} M. In addition, it benefits from a streamlined "in tube" process and is relatively rapid (≈30 min), suggesting the potential for point-of-care applications.

4.3. Surface-Enhanced Raman Scattering

Raman spectroscopy enables the identification of chemical bonds and structures in a sample by irradiating it with a laser beam and collecting the inelastic scattered photons with a detector. In this way, the spectroscopy technique enables the identification of molecules through their molecular fingerprints observed in Raman spectra and, consequently, biological sample characterization with minimal or no preprocessing activity.

Raman scattering signals are intrinsically weak, but they can be significantly enhanced by factors beyond 10^{16} when molecules are adsorbed on a roughened metal surface due to two complementary mechanisms, i.e., electromagnetic enhancement and chemical enhancement. By combining Raman spectroscopy and signal amplification mediated by plasmonic nanostructures, SERS spectroscopy is becoming a powerful analytical tool in the field of cell and molecular biology owing to its detection sensitivity down to the single-molecule level and multiplexing capability.

In the life science applications of SERS, two detection strategies are commonly used: one is label-free, and one is based on the indirect use of so-called SERS tags, that is, metal NPs with adsorbed Raman probe molecules (Raman reporters) on the surface that are functionalized by antibodies or other ligands.

Both label-free and indirect SERS detection have been extensively studied in the context of liquid biopsies for analyzing samples where CTCs, exosomes, ctDNA, cell-free RNAs, and protein cancer biomarkers are dispersed.

Quantitative detection of CTCs with an LoD down to 1 cell mL^{-1} has been achieved with and without an enrichment step before SERS spectroscopy using several approaches, including a combination of targeted SERS NPs with magnetic enrichment, and Au nanostars-based SERS tags.[179–187] Multiplexed detection of CTCs has also demonstrated a very accurate discrimination of CTCs by using up to four recognition ligands.[188,189]

One of the most promising recent results in the field of SERS-based analysis of CTCs is the possibility of characterizing the phenotypic evolution of the cells during pharmacological treatment.[190] In particular, the SERS-based technique based on antibody-conjugated and Raman reporter-coated AuNPs with a diameter of 60 nm, is able to characterize the phenotypic changes of CTCs from stage-IV melanoma patients receiving immunological or molecular targeted therapies. The working principle of the technique includes a preliminary step for removing red blood cells and leukocytes by density gradient centrifugation and CD45 depletion, respectively. Then, the remaining cells are incubated with the four different antibody-conjugated SERS labels, and then simultaneously detected by Raman spectroscopy using a portable Raman microscope available on the market, using an integration time of 1 s and a laser power of 70 mW at 785 nm. The method has three key advantages over some of the well-established technologies, e.g., the CellSearch system. It is i) extremely sensitive (10 cells in 10 mL of blood), ii) highly multiplexed (it involves the simultaneous monitoring of several surface protein expression profiles), and iii) simple (because it does not require the initial enrichment of CTCs).

Complex SERS-based analysis systems for CTC capture, enrichment, detection with LoD down to 1 cell mL^{-1}, and release

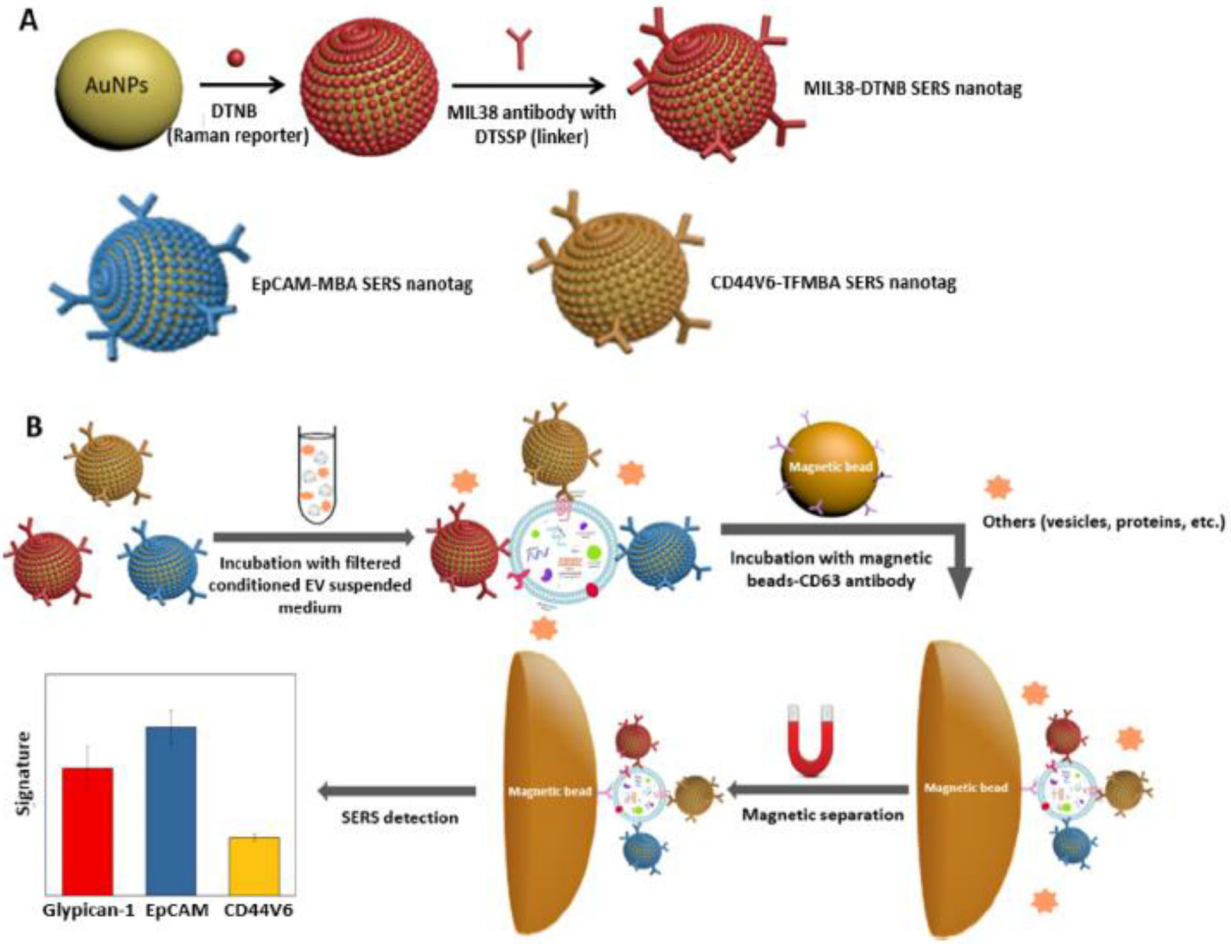

Figure 6. SERS-based method for phenotypic profiling of cancer-derived small extracellular vesicles. A) Nanotags preparation. B) SERS nanotags and CD63 antibody-functionalized magnetic beads for molecular phenotype profiling of CD63-positive EVs. Reproduced with permission.[197] Copyright 2020, American Chemical Society.

have been reported in the literature.[191,192] They exploited either a combination of metal and superparamagnetic NPs or SERS-active magnetic NPs.

As established by some recently published findings, SERS tags can be successfully applied to the detection of tumor-derived exosomes and their sensitive phenotypic profiling.[193–197] In particular, rapid and multiplexed phenotypic profiling of exosomes secreted by a human pancreatic carcinoma cell line (Panc-1 cells), has been proved to form a sandwich immunoassay by using both specific detection antibody-coated SERS nanotags and capture antibody (CD63)-conjugated magnetic beads.[197] As shown in **Figure 6**, SERS nanotags are AuNPs to which small organic molecules serving as Raman reporter molecules are covalently bound. Antibodies for the selective recognition of the three selected biomarkers, that is Glypican-1, EpCAM, and CD44 variant isoform 6 (CD44V6), are conjugated on the NP surface. The AuNPs were dispersed in the medium where the exosomes were suspended and, after the first incubation step, a second incubation step with the functionalized magnetic beads takes place. Molecular phenotype profiling was performed by SERS detection after magnetic separation. A commercially available portable Raman microscope excites the samples by a laser beam at 785 nm with a power of 15 mW to acquire the Raman spectra (integration time = 10 s). The LoD of the method is a few million exosomes per mL.

Several approaches for label-free SERS detection of exosomes have been developed.[198,199] These techniques use statistical methods to identify tumor-specific spectral signatures with good accuracy values. For example, an accuracy of 90% in differentiating exosomes originating from pancreatic cancer and exosomes from normal pancreatic epithelial cell lines has been reported by Carmicheal et al., who carried out SERS measurements using a commercial confocal Raman microscope with 785 nm diode laser excitation (laser power = 10 mW).[203]

Some promising results on ctDNA detection by SERS have been recently reported. In particular, femtomolar and sub-femtomolar LoD values have been demonstrated for ctDNA detection by enzymatic amplification combined with SERS tags.[200,201] By combining SERS and PCR, an assay detecting three clinically important melanoma DNA mutations in ctDNA has been recently developed with a sensitivity and accuracy similar to that of droplet digital PCR (ddPCR).[16]

Only a few experiments on label-free SERS detection of cfmiRNA have been reported in the literature, while most SERS-based approaches for miRNA detection exploit SERS tags[202–205] The record LoD of 0.85×10^{-18} M has been obtained by a complex core–satellite nanostructure including a plasmonic Au nanodumbbel as the core and Au NPs as satellites.[206] The nanostructures assembly is triggered by the target miRNA (miRNA-1246) and switches on the SERS signal, according to a "off-to-on" SERS strategy.

SERS-based ultrasensitive and multiplexed detection of cancer-related proteins is the topic of a well-established research effort for at least one decade. This effort aims at demonstrating detection techniques having a better LoD and higher multiplexing capabilities with respect to ELISA assays. Different mechanisms have been experimented, including those exploiting formation of a sandwich structure generating a SERS signal or dissociation of core–satellite assemblies inducing SERS signal turn "off." Li et al. reported an interesting example of immunosensor having a very good LoD value (7 fg mL^{-1}) that has been experimented in the context of protein cancer biomarker detection.[207] The sensor was successfully used for detection of the vascular endothelial growth factor in the human blood plasma from clinical breast cancer patient samples.

5. Miniaturized Platforms Based on Optical Resonators

There are three main optical microresonator systems that can be used for liquid biopsies: i) whispering gallery mode (WGM) optical resonators, ii) photonic crystal resonators, and iii) Fabry–Perot interferometers. These three technologies are platform systems, meaning that although they can be used for liquid biopsies, they can also be tailored for other sensing applications.

WGM optical resonators are ultrasensitive, rapid, and label-free biochemical sensors. Owing to their small size (down to micron scale), they can be incorporated into miniaturized and economical sensing platforms. WGM resonators have been used to sense a wide variety of biological analytes, including single macromolecules, viruses, exosomes, ribosomes, 8-mer oligonucleotides, and atomic ions.[208–212] Unlike other label-free sensing systems such as SPR, which can take hours to days to take measurements, micro/nano optical resonators can perform sensing in <30 s.[213,214] These resonators derive their sensitivity and quick response time from the resonant recirculation of light. Light is evanescently coupled into WGM resonators using an optical fiber, waveguide, or prism and then "trapped" inside the resonator via total internal reflection.[208,211,215–216] This is analogous to how light travels through an optical fiber, but one that has been bent into a ring. As such, light continuously circulates within the device. The input light source is typically a tunable laser, although light-emitting diodes have been used as well.[217]

At particular wavelengths, known as resonance wavelengths, constructive interference occurs upon each roundtrip, causing a buildup of light within the resonator. The resonance condition is given by $2\pi r\, n_{\text{eff}} = m\lambda$, where r is the distance from the center of revolution, n_{eff} is the effective refractive index of the propagating mode, λ is the resonance wavelength, and m is the azimuthal mode number of light propagating within the resonator. As the mode (electric field distribution) is concentrated near the outer edge of the resonator, the radial coordinate is typically chosen as the radius of the outer circumference of the resonator. Optical resonators used for biosensing are usually fairly large (≈100 µm in diameter), so the azimuthal mode number for visible light is typically $m \approx 10^2$ or greater. These large mode numbers correspond to higher quality factors (Q) as there is less bending loss compared to smaller devices operating at a smaller mode number. The Q-factor can be defined as $\lambda/\Delta\lambda$, where $\Delta\lambda$ is the full width at half maximum of the resonance. The Q-factor is one figure of merit for these sensors. Higher Q-factors correspond to longer photon storage lifetimes, which in turn correspond to lower limits of detection and higher resolution in analyte concentration measurements because smaller spectral shifts can be resolved. The effective refractive index of the particular mode can be obtained through finite element simulations or, analytically, in the case of a simple microsphere or cylinder.

As analyte particles bind to the surface of an optical resonator, they induce a resonance frequency change. This change in resonance frequency is due to an increase in the optical path length, which is a product of the refractive index of the medium and the geometric path length of the light. Although light primarily circulates within the resonator, part of the light evanesces outside the resonator (≈100 nm) and can interact with the analyte molecules. As such, WGM sensors are very sensitive refractive index sensors. The resonance frequency change of the optical microcavity upon analyte binding is monitored by tracking dips in the transmission of the optical fiber or waveguide that occurs at the resonance wavelength. These dips occur because, at resonance, light coupling out from the resonator and back into the fiber/waveguide destructively interferes with any light that comes directly down the fiber/waveguide from the source laser. Alternatively, one can explain this dip as power being primarily coupled into the resonator as opposed to simply transmitting the optical fiber. A tunable wavelength laser was used to locate the resonance. For biosensing experiments, the wavelength of the laser is usually chosen to be in the visible range, where absorption of light by water is minimized.[218]

The sensitivity of WGM optical resonators can be further increased by coupling them to plasmonic particles such as gold nanorods or trimers.[219] This occurs because the evanescent field of an optical microcavity resonator can excite localized LSPR of a plasmonic particle, thus generating an enhanced electric field, which can be used as a sensing hotspot. Although LSPR excitation can boost sensitivity for single-particle detection, these hybrid WGM systems have significantly less capture area than a bare device, making capture events less likely. In addition, plasmonic particles such as nanorods need to be aligned to the polarization of the cavity for maximum sensitivity. As they are currently randomly placed on these sensors, this makes their throughput very low. Their signal amplification is also often inconsistent due to fabrication nonuniformities and differing nanoparticle alignment.

The most common WGM sensor geometries used for biosensing experiments are microtoroids, microspheres, microrings, and microcylinders (optofluidic ring resonators).[208,211,220,221] Each of these geometries has particular advantages and disadvantages with regard to biochemical sensing. These resonators are fabricated from low-loss dielectric materials. Microrings, which are closed looped silicon waveguides on a chip, have the poorest

LoD of a few nanomolars. Picomolar LoDs can be obtained with ring resonators if a sandwich assay is used.[215] The advantage of microring resonators, however, is that due to their planar geometry, they are easily multiplexed, meaning that they can be fabricated in an array format enabling simultaneous experiments. Although microtoroid resonators have a ring shape, they are different and more sensitive than silicon photonic microring resonators.[220,222] This is because microtoroid resonators have a pedestal, and thus the sensing region is lifted off from the substrate, preventing light from scattering off and leaking into the substrate. In addition, this geometry permits a carbon dioxide laser reflow step, which results in an extremely smooth surface. As a result, light can be confined in the microtoroid for longer periods of time, resulting in a significantly higher *Q*-factor and more sensitive biochemical sensing than a microring. Microtoroids have a sparser mode spectrum than microspheres, which simplifies tracking of a particular mode of light inside the toroid. Because they are completely fabricated on a chip, microtoroids have multiplexing potential. Microspheres are formed by melting the tip of an optical fiber. One main advantage of microspheres is that they are easily fabricated and do not require cleanroom facilities. Similar to microtoroids, microspheres also have ultrahigh ($>10^7$) *Q*-factors. Although microspheres have been used for single-particle detection experiments, to our knowledge, they have not yet been used for liquid biopsies, although they potentially could be. As they are formed by melting the tip of an optical fiber, they are not easily multiplexable or mass producible. The degree of multiplexing that is available or possible from novel technologies is considered an important feature. Optofluidic ring resonators (OFRRs) are thin-walled glass capillaries.[223] Resonances are excited between the inner and outer diameters of the cylinder through which the analyte flows. The advantage of OFRR is that it has inherent fluidic integration. Because light is coupled to the outside of the OFRR using a tapered optical fiber and the analyte flows inside the OFRR, noise due to mechanical fluctuations of the taper during fluid flow can be reduced compared to other WGM geometries. For geometries such as toroids, alternative robust light coupling schemes have recently been proposed, such as using a nanoantenna positioned close to its surface.[223]

Because WGM optical resonators are micron-scale, they have the potential to be very compact and economical sensing systems. A complete biosensor on a chip involves not only the resonator but also an integrated light source and detector. One possible way to integrate the light source is to exploit silicon photoluminescence. Enhanced photoluminescence has been demonstrated in amorphous silicon ring resonators, which can serve as a potential on-chip light source.[224]

One WGM optical resonator system that has been used for liquid biopsy is the frequency locked optical whispering evanescent resonator (FLOWER). FLOWER is a sensing system that uses an optical microcavity, autobalanced detection, frequency-locking feedback loop, and data processing techniques to improve signal-to-noise ratio (SNR). FLOWER has been used to sense a wide variety of biological analytes, including single interleukin-2 molecules at an SNR of 5 as well as single ribosomes, and human chorionic gonadotropin in urine at a concentration of 1×10^{-15} M.[208,225] A schematic of a FLOWER is shown in **Figure 7**. As opposed to traditional microcavity sensing systems, which continuously scan the wavelength of a tunable laser to track the resonance frequency, FLOWER locks the laser wavelength to the cavity resonance. As the particles bind and perturb the resonance frequency, a feedback controller maintains the lock. This enables smaller and more transient events to be detected, which may have been missed in a conventional system with large and slow wavelength scans. An advantage of FLOWER over other single-molecule detection systems such as single-molecule array (SIMOA) is that FLOWER can provide kinetic as well as detection information.[226]

As an example of potential application in the field of liquid biopsy, FLOWER has been used to sense single tumor-derived exosomes in serum from mice.[210] Exosomes are challenging to detect; however, as they are mainly filled with water, making the index of refraction contrast very low between them and the background medium. FLOWER was used to sense single exosomes shed from human Burkitt's lymphoma cells. These cells were implanted into mice and blood was drawn from the tail vein every week for five weeks, after which the tumor had grown so large that the mouse was euthanized. FLOWER was used to track the progression of the tumor over time by sensing exosomes in the blood. Samples from later weeks generated a larger signal increase (resonance wavelength shift) than those from earlier weeks (**Figure 8**). This signal increase over time was not observed in mice with no tumor. For these experiments, light from a tunable laser was evanescently coupled into a microtoroid optical resonator using a tapered optical fiber.[208,223]

Antibodies were used to capture exosomes on the surface of the toroid. The sensing region of the microtoroid is made of silica, and so can be readily functionalized with capture agents such as DNA, aptamers, and/or antibodies for specificity. For these exosome experiments, the microtoroid was functionalized with antibodies for human CD81, a protein that is enriched in exosome membranes.[227] One advantage of FLOWER over traditional detection systems is that only a small volume (≈1–100 µL) of the sample is needed. This allows repeated blood draws from a single mouse without requiring the mouse to be sacrificed. It is important to note that in these experiments, tumor exosomes could be differentiated from exosomes shed by normal cells because a xenograft model was used (human tumor cells were placed inside a mouse).[228] However, unique exosome surface markers that can recognize healthy from cancerous patients have been discovered through mass spectrometry; thus, in principle, FLOWER could be used in conjunction with those specific surface markers for liquid biopsy assays.[229]

Because FLOWER can sense single exosomes, the magnitude of the resonance wavelength shift upon exosome binding can be checked with theory and used to confirm an exosome binding event. Another advantage of being able to measure single particle binding events is that these signals are observed as a sudden rise in the resonance wavelength that can be easily distinguished from thermal drift, which occurs slowly over a much longer time scale. The resonance wavelength shift upon particle binding is described by perturbation theory and is given by the Bethe–Schwinger cavity perturbation formula[230]

$$\frac{\Delta\omega}{\omega} \approx -\frac{\varepsilon_b \mathbf{E}_0^{\dagger} \overleftrightarrow{\alpha}(\omega)\, \mathbf{E}_0}{2\varepsilon_0 \varepsilon_r V_m \% \left|\mathbf{E}_0\right|^2_{\max}}, \quad (1)$$

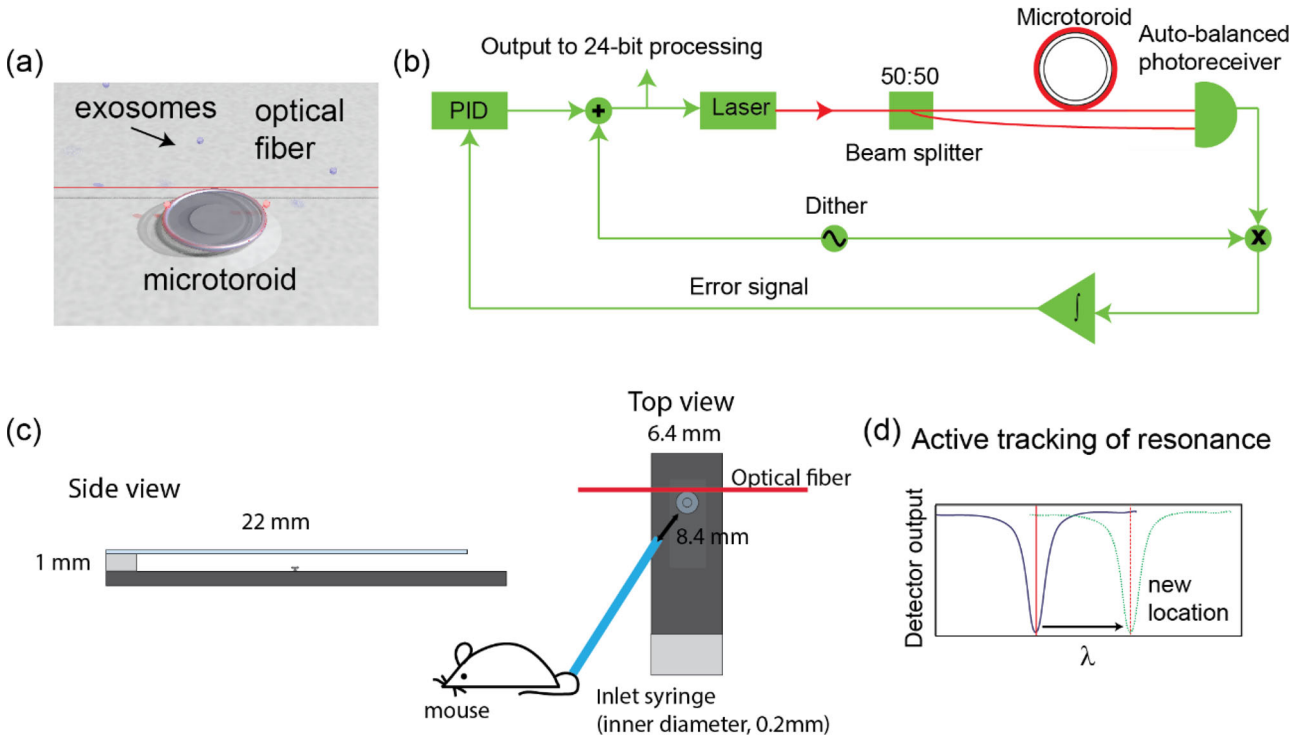

Figure 7. Overview of FLOWER. a) Artistic rendering of exosomes binding to a microtoroid optical resonator. For sensing experiments, light is evanescently coupled into the microtoroid using an optical fiber. b) Block diagram of FLOWER. Light is sent from a tunable wavelength laser to both the microtoroid and an autobalanced photoreceiver. The output of the receiver is multiplied by a dither signal to generate an error signal to determine whether the laser frequency matches the cavity resonance frequency c) Schematic of the flow cell which is used. The sample cell is open on three sides and fluid is flowed through it. d) As exosomes bind to the surface of the toroid, the resonance frequency of the toroid shifts. This is monitored via active tracking of the resonance via FLOWER. Reproduced with permission.[208] Copyright 2015, American Chemical Society.

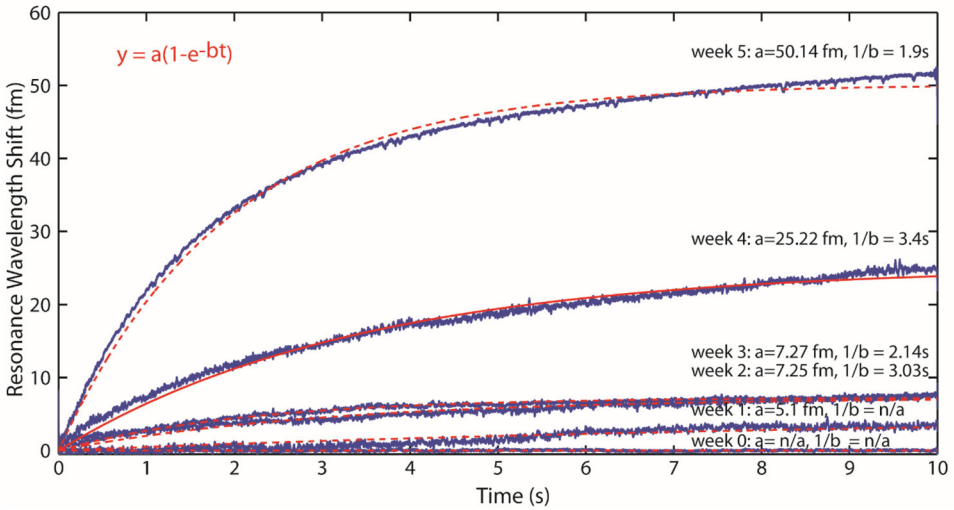

Figure 8. Exosome binding curves. Blood was taken from the tail vein of a mouse with implanted human tumor cells. Serum samples were flowed over the toroid. The resonance frequency of the microtoroid shifts in response to exosome binding. Samples from later weeks generate a larger shift, presumably due to a greater exosome concentration. The red dashed lines represent an exponential fit to the data. Reproduced with permission.[208] Copyright 2015, American Chemical Society.

where ε_0 is the permittivity of free space; ε_b is the permittivity of the background medium (for biosensing experiments, water); $\mathbf{E}_0$ is the electric field at the binding site for an unperturbed WGM; † represents the conjugate-transpose; $|\mathbf{E}_0|^2_{max}$ is the maximum intensity within the toroid; V_m is the mode volume of the resonant mode, which can be obtained through finite element simulation; ε_r is the dielectric constant of the resonator (usually silica); and $\overleftrightarrow{\alpha}(\omega)$ is the polarizability tensor of the particle. For isotropic NPs such as spheres or cubes, $\overleftrightarrow{\alpha}(\omega)$ can be treated as scalar.[231] From Equation (1), one can see that the wavelength shift upon particle binding is proportional to the polarizability of the particle. Generally, larger molecules are more polarizable and thus result in a larger frequency shift.

Microring resonators have also been used for a variety of biological applications. Although they do not achieve the attomolar concentration single-macromolecule sensitivity of microtoroid optical resonators, microring resonators possess some fabrication advantages.[208,232] With microring sensors, both the waveguide and the microring are fabricated on the chip. This enables multiplexing and the ability to subtract the signal from a reference resonator to account for thermal drift. Microring resonators have been used to sense miRNAs with an LoD of 10×10^{-12} M.[233] The possibility of using an array of properly designed microring resonators to sense a set of five serum proteins capable of predicting lung cancer with quite good accuracy has been also envisaged.[234]

The final WGM resonator systems mentioned here are OFRRs. OFRRs have been used to sense DNA methylation.[173] DNA methylation can increase the likelihood of genetic mutation, thus making it an important early cancer diagnostic biomarker.[235] In addition OFRR's have been used to sense the breast cancer biomarker HER2 at a concentration of 13 ng mL^{-1} in 30 min.[236]

The second class of optical resonators used for liquid biopsies is photonic crystal resonators. Photonic crystals are periodic dielectric nanostructures that enable reflection at specific wavelength ranges called band gaps. These wavelengths of peak reflection can shift upon changes in the refractive index caused by analyte binding.[237] Recently, a technology known as photonic resonator absorption microscopy (PRAM) was used to sense circulating exosomal miRNA.[238] miRNA-375, and −1290 have been shown to correlate with prostate cancer progression. In PRAM, AuNPs are bound to a photonic crystal, thus creating a hybrid AuNPs-photonic crystal system reminiscent of hybrid-WGM biosensing systems.[211] The resonance of the gold particle is matched to the photonic crystal resonance wavelength. This enables enhanced excitation of the AuNP and a decrease in the reflected light from the photonic crystal. A miRNA-specific DNA sequence is bound to the surface of the AuNP to enable specific binding. When miRNA binds to the DNA probes on the AuNPs, this causes a change in the resonance reflection wavelength. This reflection peak wavelength shift can be tracked for each bound AuNP, thus creating the potential for multiplexing. This is one advantage of PRAM over hybrid WGM microsphere sensing systems. PRAM was shown to have an LoD of $\approx 100 \times 10^{-18}$ M for miRNA-375 and a detection time of under 2 h.

Another photonic crystal biosensor was made from a grating coated with a high-refractive-index TiO_2 film.[239] This sensor was able to sense exosomes with an LoD of 2.18×10^9 exosomes per mL. Other types of photonic crystals, such as hollow core fibers, can potentially be used as robust and inexpensive liquid biopsy sensors that can be placed inside the body.

Fabry–Perot interferometers, or etalons, are another example of an optical resonator that can be used for liquid biopsy. A Fabry–Perot resonator is composed of two partially reflective mirrors between which light bounces back and forth. While most of the light is reflected, a small fraction of the light is transmitted through the mirrors, and the transmission spectrum can be measured using a spectrometer. Changes in the spectrum occur in response to refractive index changes as a result of the injected analyte within the cavity.[240] As a Fabry–Perot biosensor is based on the superposition of waves, and is similar in principle to microcavity optical resonator biosensors. Although Fabry–Perot biosensors typically have lower Q-factors than WGM resonators, they can be integrated with microfluidics or placed on the tip of or within an optical fiber or needle, making them robust sensors with the potential for in vivo implantation.[241] In addition, Fabry–Perot sensors are significantly less complicated to fabricate than photonic crystal cavities. The resolution of a Fabry–Perot interferometer is often determined by the resolution of the spectrometer used to measure the interference fringe shifts.

Many different ways of fabricating Fabry–Perot biosensors have been described. In one method, porous silicon was electrochemically etched to form microstructures that can generate Fabry–Perot interference fringes.[241] This porous silicon interferometric sensor was used to sense femtomolar concentrations of DNA. A single cell Fabry–Perot biosensor with a Q of around 330 was made by having two single-mode fibers face each other. The end face of each fiber had a gold reflective coating.[242] Individual cells were held in between the fiber end faces by a micropipette attached to a syringe pump. This configuration was able to sense the presence and absence of Madin Darby canine kidney cells. In addition, it was able to determine the size and refractive index of the cell to within ± 4% and ± 0.2%, respectively. Because cancerous cells have a higher refractive index (n = 1.37-1.4) than healthy cells (n = 1.35), this method could potentially be applied to sense CTCs.[243] Beyond the exosomes, miRNAs, and proteins mentioned in this section, other cancer biomarkers that have the potential to be sensed with optical resonators include mRNAs and long noncoding RNAs.[244]

Among the techniques mentioned in Section 5, only microrings have been commercialized. In the United States, there is a Clinical Laboratory Improvement Amendment (CLIA) waiver that enables laboratories to diagnose and treat patients without a very long approval process. This process can enable other technologies such as the ones mentioned in this section to be used for clinical purposes.[245]

6. Overview of Complementary and Competing Technologies

Most of the methodologies and benchtop instruments currently used in both clinical diagnostics and research activity in the field of liquid biopsies use photonics, and in particular, the physical phenomenon of fluorescence and imaging systems, in combination with other enabling technologies. The CellSearch system and Cobas EGFR Mutation Test v2 are two examples

of multi-step methodologies on the market that exploit several technological approaches, including fluorescence. The CellSearch system, which is intended for the enumeration of CTCs of epithelial origin in whole blood, uses a combination of immunomagnetic and fluorescence imaging, integrating a fluorescent microscope scanner.[246] The Cobas EGFR Mutation Test v2, which is a real-time PCR test for ctDNA-based liquid biopsy, makes use of fluorescent dyes to detect target DNA.[247] Most of the third-generation long-range DNA sequencing and mapping technologies such as those commercialized by Illumina and Pacific Biosciences (PacBio), which are widely used in the context of liquid biopsies also enabling promising tests such as Galleri by Grail that is intended for multi-cancer detection and localization using methylation signatures in cell-free DNA, uses fluorescence for detection.[248–250] For example, the PacBio SMRT technology sequences DNA using sequencing-by-synthesis, and optically monitors fluorescently tagged nucleotides as they are incorporated into individual template molecules.[251,252] Even one of the most used platforms for detecting point mutations in ctDNA, the ddPCR implemented in the commercial QX 200 system, utilizes fluorescence measurements to determine which droplets contain a nucleic acid target..[253]

Aiming at miniaturizing the bioanalytical tools for liquid biopsy, microfluidics has demonstrated promising potential, especially for the separation of CTCs from whole blood, ctDNA/miRNA extraction, and exosome isolation.[254–259] An example of a microfluidic platform for liquid biopsies is the CTC-iChip.[260] This is an improvement over a previous system known as a micropost-CTC chip.[261] CTCs are bound to the surface of micropillars/posts, which are functionalized with EpCAM antibodies. The flow characteristics of the micropost CTC chip are optimized to maximize the contact time between a CTC and a micropost. In one formulation, herringbone grooves are used to create vortices that can further drive CTCs to a micropost.[262] The CTC-iChip combines an inertial focusing microfluidic CTC capture platform with magnetic bead-based cell sorting technology. This eliminates the need for antibody-functionalized microposts, which previously prevented captured cells from being analyzed in subsequent assays. In the first step, red blood cells, platelets, free magnetic beads, and plasma are removed by hydrodynamic-based size sorting. In the second step, white blood cells and CTCs are ordered in a row along a streamline via inertial focusing. This facilitates the third stage, when white blood cells are tagged with magnetic beads in order to magnetically deflect them away. This leaves a solution of pure CTCs which can further be analyzed with other technologies that are often fluorescence-based. The CTC-iChip was tested using breast, prostate, lung, pancreas, and colorectal cancer cells.[263] It has an assay time of 6–7 h and can sort 10^7 cells s^{-1}. The CTC-iChip capture efficiency, which scales with EpCAM expression, was reported to be 77.8% ± 7.8% for a mesenchymal breast cancer line and 98.6 ± 4.3% for SBK3 human breast cancer cells, which had more EpCAM expression.

Although there are a few interesting exceptions, most of the microfluidics chips intended for liquid biopsies still require external and complex instrumentation in applications outside a controlled laboratories.[264] As demonstrated by several lab-on-chip microsystems reported in the literature, microfluidics and micro and nanophotonics/plasmonics are highly compatible technologies that could be smartly integrated to implement photonic (or optofluidic) lab-on-chip microsystems that integrate biomarker quantitative detection.[265]

Nanomechanical assays typically exploiting the deflection of a cantilever to detect target biomarkers are emerging as a powerful tool in the field of analytical biochemistry. Etayash et al. reported an interesting example of a nanomechanical assay for exosome detection.[266] The sensing platform is based on a cantilever array simultaneously detecting multiple exosomal surface-antigens. The achieved LoD is 200 exosomes per mL, and the cantilever deflection is measured by a photonic setup including a laser source and position-sensitive detector.

A notable class of assays for liquid biopsies that do not use photonics are those relying on electrochemical approaches, such as several electrochemical platforms for exosomes, miRNA, and protein detection reported in the last few years. An LoD $<10^5$ exosomes was achieved by a magneto-electrochemical assay carried out in an eight-channel integrated platform (iMEX) including eight potentiostats (each having three electrodes: reference, counter, and working), an 8-to-1 multiplexer, an analog-to-digital converter, a digital-to-analog converter, and a microcontroller unit (**Figure 9**).[267] A significant LoD improvement down to 100 exosomes per mL has been obtained by a more complex assay using quantum dots as signal amplifiers.[268]

Electrochemical detection of miRNA through voltammetric, amperometric, and impedimetric methods is usually based on hybridization between the target miRNA and the receptor probe that is bound on the electrode surface.[269,270] Electrocatalytic amplification was used to enhance the LoD, achieving values down to 80×10^{-15} M.[271] Electrochemical detection of cancer biomarker proteins is currently a promising research area, with the best achieved LoD values of the order of a few fg mL^{-1}, and widely experimentally demonstrated multiplexing capability.[272]

7. Conclusion

Bioanalytical technologies for cell and molecule analysis are improving, particularly for the analysis of mutations at the DNA level. Consequently, more data on the clinical utility of circulating cancer biomarkers are available. Liquid biopsies are becoming a part of routine clinical diagnostics, introducing important changes in the treatment of cancer patients.

In turn, clinical and translational medicine interest in liquid biopsies is stimulating an increase in research efforts on enabling technologies that are typically very complex, as they involve a plurality of biochemical and physical phenomena. In addition, liquid biopsies typically generate big data sets whose processing is still challenging, despite recent progresses in the field of machine learning algorithms for data analytics.

Research activity on liquid biopsy technologies currently has two major targets: i) performance improvement of bioanalytical assays in terms of LoD, throughput, multiplexing capability, duration, selectivity, and specificity and ii) miniaturization of bioanalytical systems and cost/complexity reduction, in order to develop liquid biopsies that are realistically feasible at the point-of-care level.

Owing to the achievements critically discussed in this paper, we believe that nanoscopy, nanoplasmonics, and integrated micro and nanophotonics can play a pivotal role in the field of

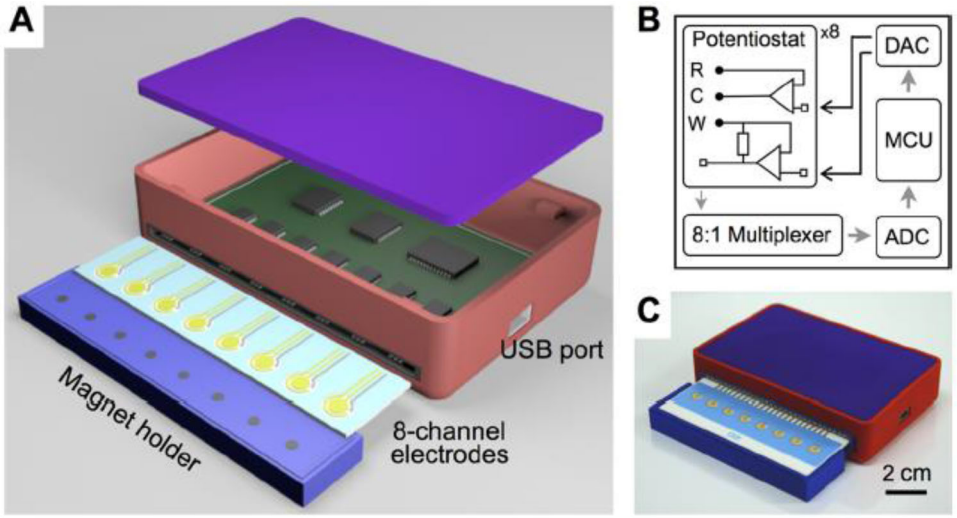

Figure 9. iMEX platform with a schematic illustration of its components A), a diagram of the readout circuit B), and a rendering of the packaged device C). Reproduced with permission.[267] Copyright 2016, American Chemical Society.

Table 1. Promising emerging photonic technologies intended for liquid biopsies.

	Circulating biomarkers					
Emerging photonic technologies	CTCs	ctDNA	Cancer-derived exosomes	Cell-free RNA	Cell-free proteins	TEPs
High-speed high-resolution fluorescence microscopy	Qualitative/quantitative analysis of subcellular structures having nanometer size.		Super-resolution imaging and extraction of phenotypic information.[124]			Super-resolution imaging
SPR/iSPR			Detection (also w/o purification) with LoD ranging from 5000 to 10 0000 exosomes per μL.[157,159,161]	Detection of miRNA with LoD of 1×10^{-18} M.[166]	Detection with LoD of the order of 100 pg mL^{-1}.[169]	
LSPR			Single exosome detection.[174]	Detection of miRNA with LoD of $\approx 0.2 \times 10^{-15}$ M.[178]		
SERS	i) Detection with a LoD down to 1 cell mL^{-1}.[179–187] ii) Characterization of phenotypic evolution during the pharmacologic treatment.[190]	i) Detection with LoD $< 1 \times 10^{-15}$ M.[200,201] ii) Mutation identification (in combination with PCR).[16]		Detection of miRNA with LoD $< 0.1 \times 10^{-15}$ M.[206]	Detection with LoD of the order of 1–10 fg mL^{-1}.[207]	
WGM/PhC optical resonators			Single exosome detection.[208]	Detection of miRNA with LoD of 10×10^{-12} M.[233]	Detection with LoD of the order of 1–10 ng mL^{-1}.[236]	
Most promising complementary/competing technology	Detection by microfluidic chips in combination with other fluorescence-based technologies.		Detection by quantum-dots based electrochemical assay with LoD of 100 exosomes mL.[268]	Electrochemical detection of miRNA with LoD of 80×10^{-15} M.[271]	Electrochemical detection with LoD of the order of a few fg mL^{-1}[272]	

advanced liquid biopsy technologies, if they will fully demonstrate their potential to be superior over the well-established methodologies in terms of instrument complexity, cost, and size. Currently, sample preprocessing is a critical task in all liquid biopsies and market success of the above-mentioned emerging technologies may be strongly correlated to their capability to reduce the critical aspects associated to that task.

The most promising emerging photonic technologies intended for liquid biopsies are mapped in **Table 1**, alongside some complementary/competitive technologies. These technologies

are typically at medium-low TRL (≤5), while high-TRL instruments and techniques have already been discussed in Section 2 and summarized in Figure 1.

The spatial resolution of nanoscopy techniques, currently in the order of a few tens of nanometers, is quickly improving. With the approaches at the state-of-the-art, CTCs, tumor-derived exosomes, and TEPs can be imaged, and their internal biological structures can be dynamically studied together with their interaction mechanisms with the outer environment. Fluorescence microscopy, which is a key tool for the vast majority of instruments currently utilized for liquid biopsies, is likely to retain this crucial role and decisively contribute to the definitive understanding of metastatic development biology.

A few studies suggest that nanoscopy performance can be improved by using optical tweezers to trap the biological target under analysis. Free-space and chip-scale optical trapping combined with super-resolution fluorescence microscopy could be particularly useful in the context of liquid biopsies to enable trapping and analysis of micrometric and sub-micrometric biologic structures.

SERS-based platforms in combination with microfluidics have the potential to become a miniaturized alternative to the bulk instruments currently used for CTC enumeration/characterization, ctDNA targeted detection with sub-femtomolar LoD, and protein biomarkers sensing.

Nanoplasmonics and microphotonics have both demonstrated their potential to detect cancer-derived exosomes with a resolution down to the single exosome, and new translational studies are needed to assess both the clinical utility of exosome quantitative detection and the possibility of using these technologies in clinical practice.

The degree of multiplexing potentially achievable by the emerging technologies for liquid biopsies is a key feature that could considerably impact on their application in medical diagnostics. SPRi, SERS, and microring resonator technologies have already demonstrated interesting multiplexing capability and seem the most promising from this point of view.

Quantitative detection of a target cfmiRNA molecule can be implemented by several photonic technologies at the micro and nanoscale. The best LoD value to our knowledge ($<0.1 \times 10^{-15}$ M) has been achieved by SERS; however, SERS application in the context of cfmiRNA detection now needs further validation studies.

Highly multiplexed sensing of properly selected protein biomarker panels may be very useful in the context of liquid biopsies and several emerging photonic technologies, mainly WGM resonators and nanoplasmonic structures, are being experimented in this field.

TEPs-based liquid biopsies represent a quite unexplored research field, especially from the technological point of view. If the clinical utility of this class of liquid biopsies can be fully demonstrated, several technological research advances could start soon.

From the medical point of view, there is no doubt on the role of liquid biopsies as a new way to get information on the molecular alteration of tumor tissue. From the technological point of view, no fully automated all-in-one instrument exists to carry out the multi-step procedures starting from a sample drown from the patient to provide datasets to support the clinical decision process. In addition, the instruments currently utilized are bulky, expensive, and need skilled personnel. Therefore, the most urgent technological challenges are i) TRL increase for the most promising emerging technologies for liquid biopsies through appropriate translational studies, ii) improvement in automation and integration for bioanalytic instruments intended for liquid biopsy, and iii) application of the artificial intelligence paradigm to facilitate a smart fusion of data from tissue biopsy, liquid biopsy, and medical imaging. The most fascinating long-term achievement is the integration of microfluidics and micro/nanophotonics for the development of lab-on-chip microsystems moving liquid biopsies from the highly sophisticated bioanalytical laboratory toward the general practitioner's surgery and ultimately the patient's home.

Supporting Information

Supporting Information is available from the Wiley Online Library or from the author.

Acknowledgements

F.D. acknowledges funding from the Italian Ministry of Education, University and Research (MIUR) under the "Fondo di finanziamento per le attività base di ricerca (FFABR)" initiative. J.S. acknowledges partial financial support from the NIH R03AG055020, R21MH111109, NSF 1842045, Gordon & Betty Moore Foundation (Grant GBMF7555.14), Flinn Foundation (Grant 26223) Arizona Alzheimer's Consortium, Barrett Cancer Imaging Grant, the Partnership for Clean Competition (2016R2000218G), and the University of Arizona Cancer Center. T.H. acknowledges funding from the European Union's Horizon 2020 research and innovation program under the Marie Sklodowska-Curie Grant Agreement No. 766181, project "DeLIVER," as well as by the Deutsche Forschungsgemeinschaft (DFG, German Science Foundation) - project number 415832635. C.A-.P. acknowledges funding from The National Institute of Cancer (INCa, http://www.e-cancer.fr), SIRIC Montpellier Cancer Grant INCa_Inserm_DGOS_12553 and ELBA - Innovative Training Networks (ITN) H2020 - European Liquid Biopsies Academy project - H2020-MSCA-ITN-2017 (http://elba.uni-plovdiv.bg) and the ERA-NET TRANSCAN 2 JTC 2016 PROLIPSY. L.E.C.-H. acknowledges funding from ELBA - Innovative Training Networks (ITN) H2020 - European Liquid Biopsies Academy project - H2020-MSCA-ITN-2017 (http://elba.uni-plovdiv.bg). V.S. acknowledges funding from the Italian Ministry of Education, University and Research (MIUR) to the Department of Molecular Medicine of the University of Pavia under the "Dipartimenti di Eccellenza (2018–2022)" initiative.

Conflict of Interest

Judith Su owns a financial stake in Femtorays Technologies which develops label-free molecular sensors.

Keywords

liquid biopsies, oncologyoptical microscopy, plasmonics, whispering gallery modes

Received: June 19, 2020
Revised: November 3, 2020
Published online:

[1] K. Pantel, C. Alix-Panabières, *Trends Mol. Med.* **2010**, *16*, 398.
[2] K. Pantel, C. Alix-Panabières, *Nat. Rev. Clin. Oncol.* **2019**, *16*, 409.

[3] Z. Eslami-S, L. E. Cortés-Hernández, L. Cayrefourcq, C. Alix-Panabières, *Cold Spring Harbor Perspect. Med.* **2020**, *10*, a037333.
[4] F.-C. Bidard, D. J. Peeters, T. Fehm, F. Nolé, R. Gisbert-Criado, D. Mavroudis, S. Grisanti, D. Generali, J. A. Garcia-Saenz, J. Stebbing, C. Caldas, P. Gazzaniga, L. Manso, R. Zamarchi, A. F. de Lascoiti, L. De Mattos-Arruda, M. Ignatiadis, R. Lebofsky, S. J. van Laere, F. Meier-Stiegen, M.-T. Sri, J. Vidal-Martinez, E. Politaki, F. Consoli, A. Bottini, E. Diaz-Rubio, J. Krell, S.-J. Dawson, C. Raimondi, A. Rutten, W. Janni, E. Munzone, V. Carañana, S. Agelaki, C. Almici, L. Dirix, E.-F. Solomayer, L. Zorzino, H. Johannes, J. S. Reis-Filho, K. Pantel, J.-Y. Pierga, S. Michiels, *Lancet Oncol.* **2014**, *15*, 406.
[5] F.-C. Bidard, *Clinical Research*, American Association for Cancer Research, USA **2019**.
[6] C. Alix-Panabières, S. Mader, K. Pantel, *J. Mol. Med.* **2017**, *95*, 133.
[7] A. Soler, L. Cayrefourcq, T. Mazard, A. Babayan, P.-J. Lamy, S. Assou, E. Assenat, K. Pantel, C. Alix-Panabières, *Sci. Rep.* **2018**, *8*, 15931.
[8] L. E. Cortés-Hernández, Z. Eslami-S, K. Pantel, C. Alix-Panabières, *Clin. Chem.* **2020**, *66*, 97.
[9] E. S. Antonarakis, C. Lu, H. Wang, B. Luber, M. Nakazawa, J. C. Roeser, Y. Chen, T. A. Mohammad, Y. Chen, H. L. Fedor, T. L. Lotan, Q. Zheng, A. M. De Marzo, J. T. Isaacs, W. B. Isaacs, R. Nadal, C. J. Paller, S. R. Denmeade, M. A. Carducci, M. A. Eisenberger, J. Luo, *N. Engl. J. Med.* **2014**, *371*, 1028.
[10] C. Hille, T. M. Gorges, S. Riethdorf, M. Mazel, T. Steuber, G. Von Amsberg, F. König, S. Peine, C. Alix-Panabières, K. Pantel, *Cells* **2019**, *8*, 1067.
[11] M. Mazel, W. Jacot, K. Pantel, K. Bartkowiak, D. Topart, L. Cayrefourcq, D. Rossille, T. Maudelonde, T. Fest, C. Alix-Panabières, *Mol. Oncol.* **2015**, *9*, 1773.
[12] L. E. Cortés-Hernández, Z. Eslami-S, C. Alix-Panabières, *Mol. Aspects Med.* **2020**, *72*, 100816.
[13] M. Elazezy, S. A. Joosse, *Comput. Struct. Biotechnol. J.* **2018**, *16*, 370.
[14] D. K. Jeppesen, A. M. Fenix, J. L. Franklin, J. N. Higginbotham, Q. Zhang, L. J. Zimmerman, D. C. Liebler, J. Ping, Q. Liu, R. Evans, W. H. Fissell, J. G. Patton, L. H. Rome, D. T. Burnette, R. J. Coffey, *Cell* **2019**, *177*, 428.
[15] M. J. Mosko, A. A. Nakorchevsky, E. Flores, H. Metzler, M. Ehrich, D. J. van den Boom, J. L. Sherwood, A. O. H. Nygren, *J. Mol. Diagn.* **2016**, *18*, 23.
[16] E. J. H. Wee, Y. Wang, S. C.-H. Tsao, M. Trau, *Theranostics* **2016**, *6*, 1506.
[17] D. Lissa, A. I. Robles, *Transl. Lung Cancer Res.* **2016**, *5*, 492.
[18] M. Théry, M. Bornens, *Curr. Opin. Cell Biol.* **2006**, *18*, 648.
[19] R. P. Alexer, N.-T. Chiou, K. M. Ansel, *Protocol Exchange* **2016**, https://doi.org/10.1038/protex.2016.057.
[20] C. Théry, K. W. Witwer, E. Aikawa, M. J. Alcaraz, J. D. Anderson, R. Andriantsitohaina, A. Antoniou, T. Arab, F. Archer, G. K. Atkin-Smith, D. C. Ayre, J.-M. Bach, D. Bachurski, H. Baharv, L. Balaj, S. Baldacchino, N. N. Bauer, A. A. Baxter, M. Bebawy, C. Beckham, A. Bedina Zavec, A. Benmoussa, A. C. Berardi, P. Bergese, E. Bielska, C. Blenkiron, S. Bobis-Wozowicz, E. Boilard, W. Boireau, A. Bongiovanni, et al., *J. Extracell. Vesicles* **2018**, *7*, 1535750.
[21] R. J. Lobb, M. L. Hastie, E. L. Norris, R. van Amerongen, J. J. Gorman, A. Möller, *Proteomics* **2017**, *17*, 1600432.
[22] R. M. Johnstone, M. Adam, J. R. Hammond, L. Orr, C. Turbide, *J. Biol. Chem.* **1987**, *262*, 9412.
[23] A. A. Sabo, G. Birolo, A. Naccarati, M. P. Dragomir, S. Aneli, A. Allione, M. Oderda, M. Allasia, P. Gontero, C. Sacerdote, P. Vineis, G. Matullo, B. Pardini, *Cancers* **2020**, *12*, 1507.
[24] A. Nanou, M. C. Miller, L. L. Zeune, S. de Wit, C. J. A. Punt, H. J. M. Groen, D. F. Hayes, J. S. de Bono, L. W. M. M. Terstappen, *Br. J. Cancer* **2020**, *122*, 801.
[25] M. Mathieu, L. Martin-Jaular, G. Lavieu, C. Théry, *Nat. Cell Biol.* **2019**, *21*, 9.
[26] C. Théry, K. W. Witwer, E. Aikawa, M. J. Alcaraz, J. D. Anderson, R. Andriantsitohaina, A. Antoniou, T. Arab, F. Archer, G. K. Atkin-Smith, D. C. Ayre, J.-M. Bach, D. Bachurski, H. Baharvand, L. Balaj, S. Baldacchino, N. N. Bauer, A. A. Baxter, M. Bebawy, C. Beckham, A. Bedina Zavec, A. Benmoussa, A. C. Berardi, P. Bergese, E. Bielska, C. Blenkiron, S. Bobis-Wozowicz, E. Boilard, W. Boireau, A. Bongiovanni, et al., *J. Extracell. Vesicles* **2018**, *7*, 1535750.
[27] P. Li, M. Kaslan, S. H. Lee, J. Yao, Z. Gao, *Theranostics* **2017**, *7*, 789.
[28] A. N. Böing, E. van der Pol, A. E. Grootemaat, F. A. W. Coumans, A. Sturk, R. Nieuwl, *J. Extracell. Vesicles* **2014**, *3*, 23430.
[29] G. Vergauwen, B. Dhondt, J. van Deun, E. De Smedt, G. Berx, E. Timmerman, K. Gevaert, I. Miinalainen, V. Cocquyt, G. Braems, R. van den Broecke, H. Denys, O. De Wever, A. Hendrix, *Sci. Rep.* **2017**, *7*, 2704.
[30] R. Kalluri, V. S. LeBleu, *Science* **2020**, *367*, eaau6977.
[31] M. Wu, Y. Ouyang, Z. Wang, R. Zhang, P.-H. Huang, C. Chen, H. Li, P. Li, D. Quinn, M. Dao, S. Suresh, Y. Sadovsky, T. J. Huang, *Proc. Natl. Acad. Sci. USA* **2017**, *114*, 10584.
[32] M. He, Y. Zeng, *J. Lab. Autom.* **2016**, *21*, 599.
[33] A. K. Krug, D. Enderle, C. Karlovich, T. Priewasser, S. Bentink, A. Spiel, K. Brinkmann, J. Emenegger, D. G. Grimm, E. Castellanos-Rizaldos, J. W. Goldman, L. V. Sequist, J.-C. Soria, D. R. Camidge, S. M. Gadgeel, H. A. Wakelee, M. Raponi, M. Noerholm, J. Skog, *Ann. Oncol.* **2018**, *29*, 700.
[34] D. J. Cha, J. L. Franklin, Y. Dou, Q. Liu, J. N. Higginbotham, M. Demory Beckler, A. M. Weaver, K. Vickers, N. Prasad, S. Levy, B. Zhang, R. J. Coffey, J. G. Patton, *Elife* **2015**, *4*, e07197.
[35] A. H. Alhasan, A. W. Scott, J. J. Wu, G. Feng, J. J. Meeks, C. S. Thaxton, C. A. Mirkin, *Proc. Natl. Acad. Sci. USA* **2016**, *113*, 10655.
[36] D. Bhagirath, T. L. Yang, N. Bucay, K. Sekhon, S. Majid, V. Shahryari, R. Dahiya, Y. Tanaka, S. Saini, *Cancer Res.* **2018**, *78*, 1833.
[37] A. Thind, C. Wilson, *J. Extracell. Vesicles* **2016**, *5*, 31292.
[38] T. Vagner, C. Spinelli, V. R. Minciacchi, L. Balaj, M. Zandian, A. Conley, A. Zijlstra, M. R. Freeman, F. Demichelis, S. De, E. M. Posadas, H. Tanaka, D. Di Vizio, *J. Extracell. Vesicles* **2018**, *7*, 1505403.
[39] S. Bratulic, F. Gatto, J. Nielsen, *Regener. Eng. Transl. Med.* **2019**, https://doi.org/10.1007/s40883-019-00141-2.
[40] H. Schwarzenbach, N. Nishida, G. A. Calin, K. Pantel, *Nat. Rev. Clin. Oncol.* **2014**, *11*, 145.
[41] P. S. Mitchell, R. K. Parkin, E. M. Kroh, B. R. Fritz, S. K. Wyman, E. L. Pogosova-Agadjanyan, A. Peterson, J. Noteboom, K. C. O'Briant, A. Allen, D. W. Lin, N. Urban, C. W. Drescher, B. S. Knudsen, D. L. Stirewalt, R. Gentleman, R. L. Vessella, P. S. Nelson, D. B. Martin, M. Tewari, *Proc. Natl. Acad. Sci. USA* **2018**, *105*, 10513.
[42] P. S. Mitchell, R. K. Parkin, E. M. Kroh, B. R. Fritz, S. K. Wyman, E. L. Pogosova-Agadjanyan, A. Peterson, J. Noteboom, K. C. O'Briant, A. Allen, D. W. Lin, N. Urban, C. W. Drescher, B. S. Knudsen, D. L. Stirewalt, R. Gentleman, R. L. Vessella, P. S. Nelson, D. B. Martin, M. Tewari, *Proc. Natl. Acad. Sci. USA* **2008**, *105*, 10513.
[43] M. A. Cortez, C. Bueso-Ramos, J. Ferdin, G. Lopez-Berestein, A. K. Sood, G. A. Calin, *Nat. Rev. Clin. Oncol.* **2011**, *8*, 467.
[44] S. Anfossi, A. Babayan, K. Pantel, G. A. Calin, *Nat. Rev. Clin. Oncol.* **2018**, *15*, 541.
[45] T. Kiss, *Cell* **2002**, *109*, 145.
[46] M. T. Bohnsack, K. E. Sloan, *Biol. Chem.* **2018**, *399*, 1265.
[47] T. Kitagawa, K. Taniuchi, M. Tsuboi, M. Sakaguchi, T. Kohsaki, T. Okabayashi, T. Saibara, *Mol. Oncol.* **2019**, *13*, 212.
[48] A. M. Schmitt, H. Y. Chang, *Cancer Cell* **2016**, *29*, 452.
[49] J. Lonsdale, J. Thomas, M. Salvatore, R. Phillips, E. Lo, S. Shad, R. Hasz, G. Walters, F. Garcia, N. Young, B. Foster, M. Moser, E. Karasik, B. Gillard, K. Ramsey, S. Sullivan, J. Bridge, H. Magazine, J. Syron, J. Fleming, L. Siminoff, H. Traino, M. Mosavel, L. Barker, S. Jewell, D. Rohrer, D. Maxim, D. Filkins, P. Harbach, E. Cortadillo, B. Berghuis, L. Turner, E. Hudson, K. Feenstra, L. Sobin, J. Robb,

P. Branton, G. Korzeniewski, C. Shive, D. Tabor, L. Qi, K. Groch, S. Nampally, S. Buia, A. Zimmerman, A. Smith, R. Burges, K. Robinson, K. Valentino, D. Bradbury, M. Cosentino, N. Diaz-Mayoral, M. Kennedy, T. Engel, P. Williams, K. Erickson, K. Ardlie, W. Winckler, G. Getz, D. DeLuca, D. MacArthur, M. Kellis, A. Thomson, T. Young, E. Gelfand, M. Donovan, Y. Meng, G. Grant, D. Mash, Y. Marcus, M. Basile, J. Liu, J. Zhu, Z. Tu, N. J. Cox, D. L. Nicolae, E. R. Gamazon, H. K. Im, A. Konkashbaev, J. Pritchard, M. Stevens, T. Flutre, X. Wen, E. T. Dermitzakis, T. Lappalainen, R. Guigo, J. Monlong, M. Sammeth, D. Koller, A. Battle, S. Mostafavi, M. McCarthy, M. Rivas, J. Maller, I. Rusyn, A. Nobel, F. Wright, A. Shabalin, M. Feolo, N. Sharopova, A. Sturcke, J. Paschal, J. M. Anderson, E. L. Wilder, L. K. Derr, E. D. Green, J. P. Struewing, G. Temple, S. Volpi, J. T. Boyer, E. J. Thomson, M. S. Guyer, C. Ng, A. Abdallah, D. Colantuoni, T. R. Insel, S. E. Koester, A. R. Little, P. K. Bender, T. Lehner, Y. Yao, C. C. Compton, J. B. Vaught, S. Sawyer, N. C. Lockhart, J. Demchok, H. F. Moore, *Nat. Genet.* **2013**, *45*, 580.

[50] F. Mertens, B. Johansson, T. Fioretos, F. Mitelman, *Nat. Rev. Cancer* **2015**, *15*, 371.

[51] J. Shen, W. Kong, Y. Wu, H. Ren, J. Wei, Y. Yang, Y. Yang, L. Yu, W. Guan, B. Liu, *J. Cancer* **2017**, *8*, 434.

[52] J. W.-C. Chang, C.-L. Shih, C.-L. Wang, J.-D. Luo, C.-W. Wang, J.-J. Hsieh, C.-J. Yu, C.-C. Chiou, *Cancer Genomics Proteomics* **2020**, *17*, 91.

[53] M. D. Pasic, G. M. Yousef, E. P. Diamandis, *Clin. Biochem.* **2013**, *46*, 397.

[54] Y. Kim, J. Jeon, S. Mejia, C. Q. Yao, V. Ignatchenko, J. O. Nyalwidhe, A. O. Gramolini, R. S. Lance, D. A. Troyer, R. R. Drake, P. C. Boutros, O. J. Semmes, T. Kislinger, *Nat. Commun.* **2016**, *7*, 11906.

[55] M. J. Duffy, *Clin. Chem.* **2006**, *52*, 345.

[56] O. Bratt, H. Lilja, *Curr. Opin. Urol.* **2015**, *25*, 59.

[57] S. M. Schubert, L. M. Arendt, W. Zhou, S. Baig, S. R. Walter, R. J. Buchsbaum, C. Kuperwasser, D. R. Walt, *Sci. Rep.* **2015**, *5*, 11034.

[58] S. Loeb, W. J. Catalona, *Ther. Adv. Urol.* **2014**, *6*, 74.

[59] D. Bruzzese, C. Mazzarella, M. Ferro, S. Perdonà, P. Chiodini, G. Perruolo, D. Terracciano, *Transl. Res.* **2014**, *164*, 444.

[60] D. J. Parekh, S. Punnen, D. D. Sjoberg, S. W. Asroff, J. L. Bailen, J. S. Cochran, R. Concepcion, R. D. David, K. B. Deck, I. Dumbadze, M. Gambla, M. S. Grable, R. J. Henderson, L. Karsh, E. B. Krisch, T. D. Langford, D. W. Lin, S. M. McGee, J. J. Munoz, C. M. Pieczonka, K. Rieger-Christ, D. R. Saltzstein, J. W. Scott, N. D. Shore, P. R. Sieber, T. M. Waldmann, F. N. Wolk, S. M. Zappala, *Eur. Urol.* **2015**, *68*, 464.

[61] M. Music, M. A. J. Iafolla, A. H. Ren, A. Soosaipillai, I. Prassas, E. P. Diamandis, *Mol. Cancer Ther.* **2019**, *18*, 1844.

[62] M. Rucevic, presented at Advances in Cancer Immunotherapy, Virtual Conf., August 2020.

[63] B. Sheng, C. Qi, B. Liu, Y. Lin, T. Fu, Q. Zeng, *Sci. Rep.* **2017**, *7*, 13807.

[64] A. N. Hoofnagle, J. O. Becker, M. H. Wener, J. W. Heinecke, *Clin. Chem.* **2008**, *54*, 1796.

[65] B. Zhang, J. R. Whiteaker, A. N. Hoofnagle, G. S. Baird, K. D. Rodland, A. G. Paulovich, *Nat. Rev. Clin. Oncol.* **2019**, *16*, 256.

[66] A. Di Meo, J. Bartlett, Y. Cheng, M. D. Pasic, G. M. Yousef, *Mol. Cancer* **2017**, *16*, 80.

[67] Y. Fradet, C. Lockhard, *Can. J. Urol.* **1997**, *4*, 400.

[68] H. He, C. Han, L. Hao, G. Zang, *Oncol. Lett.* **2016**, *12*, 83.

[69] R. Rodvien, C. H. Mielke, *West. J. Med.* **1976**, *125*, 181.

[70] A. Gros, V. Ollivier, B. Ho-Tin-Noè, *Front. Immunol.* **2015**, *5*, 678.

[71] R. A. Ali, L. M. Wuescher, R. G. Worth, *Curr. Trends Immunol.* **2015**, *16*, 65.

[72] Y. Hou, N. Carrim, Y. Wang, R. C. Gallant, A. Marshall, H. Ni, *J. Biomed. Res.* **2015**, *29*, 437.

[73] M. Thomas, R. Storey, *Thromb. Haemostasis* **2015**, *114*, 449.

[74] L. F. Brass, S. L. Diamond, T. J. Stalker, *Blood Adv.* **2016**, *1*, 5.

[75] R. Leblanc, O. Peyruchaud, *Blood* **2016**, *128*, 24.

[76] R. Buettner, *J. Thorac. Dis.* **2018**, *10*, 550.

[77] G. J. Gasic, T. B. Gasic, N. Galanti, T. Johnson, S. Murphy, *Int. J. Cancer* **1973**, *11*, 704.

[78] J. F. Mustard, R. L. Kinlough-Rathbone, M. A. Packham, *Methods Enzymol.* **1989**, *169*, 3.

[79] M. Hoffman, D. M. Monroe, H. R. Roberts, *Am. J. Clin. Pathol.* **1992**, *98*, 531.

[80] J.-P. Cazenave, P. Ohlmann, D. Cassel, A. Eckly, B. Hechler, C. Gachet, *Methods Mol. Biol.* **2004**, *272*, 13.

[81] S. Amisten, in *Platelets Megakaryocytes* (Eds: J. M. Gibbins,M. P. Mahaut-Smith), Springer, New York **2012**, p. 155.

[82] M. Best, N. Sol, I. Kooi, J. Nilsson, B. Westerman, B. Ylstra, J. Dorsman, E. Smit, H. Verheul, J. Reijneveld, B. Tannous, P. Wesseling, T. Würdinger, *Clinical Research*, American Association for Cancer Research, USA **2015**, pp. LB-124.

[83] M. G. Best, P. Wesseling, T. Wurdinger, *Cancer Res.* **2018**, *78*, 3407.

[84] M. G. Best, N. Sol, I. Kooi, J. Tannous, B. A. Westerman, F. Rustenburg, P. Schellen, H. Verschueren, E. Post, J. Koster, B. Ylstra, N. Ameziane, J. Dorsman, E. F. Smit, H. M. Verheul, D. P. Noske, J. C. Reijneveld, R. J. A. Nilsson, B. A. Tannous, P. Wesseling, T. Wurdinger, *Cancer Cell* **2015**, *28*, 666.

[85] T. Wurdinger, S. G. J. G. In't Veld, M. G. Best, *Cancer Res.* **2020**, *80*, 1371.

[86] D. Roy, M. Tiirikainen, *Trends Cancer* **2020**, *6*, 78.

[87] J. D. Cohen, L. Li, Y. Wang, C. Thoburn, B. Afsari, L. Danilova, C. Douville, A. A. Javed, F. Wong, A. Mattox, R. H. Hruban, C. L. Wolfgang, M. G. Goggins, M. Dal Molin, T.-L. Wang, R. Roden, A. P. Klein, J. Ptak, L. Dobbyn, J. Schaefer, N. Silliman, M. Popoli, J. T. Vogelstein, J. D. Browne, R. E. Schoen, R. E. Brand, J. Tie, P. Gibbs, H.-L. Wong, A. S. Mansfield, J. Jen, S. M. Hanash, M. Falconi, P. J. Allen, S. Zhou, C. Bettegowda, L. A. Diaz, C. Tomasetti, K. W. Kinzler, B. Vogelstein, A. M. Lennon, N. Papadopoulos, *Science* **2018**, *359*, 926.

[88] C. Alix-Panabières, *Nature* **2020**, *579*, S9.

[89] J. Ko, S. N. Baldassano, P.-L. Loh, K. Kording, B. Litt, D. Issadore, *Lab Chip* **2018**, *18*, 395.

[90] H. Shen, T. Liu, J. Cui, P. Borole, A. Benjamin, K. Kording, D. Issadore, *Lab Chip* **2020**, *20*, 2166.

[91] A. M. Lennon, A. H. Buchanan, I. Kinde, A. Warren, A. Honushefsky, A. T. Cohain, D. H. Ledbetter, F. Sanfilippo, K. Sheridan, D. Rosica, C. S. Adonizio, H. J. Hwang, K. Lahouel, J. D. Cohen, C. Douville, A. A. Patel, L. N. Hagmann, D. D. Rolston, N. Malani, S. Zhou, C. Bettegowda, D. L. Diehl, B. Urban, C. D. Still, L. Kann, J. I. Woods, Z. M. Salvati, J. Vadakara, R. Leeming, P. Bhattacharya, C. Walter, A. Parker, C. Lengauer, A. Klein, C. Tomasetti, E. K. Fishman, R. H. Hruban, K. W. Kinzler, B. Vogelstein, N. Papadopoulos, *Science* **2020**, *369*, eabb9601.

[92] C. Alix-Panabières, K. Pantel, *Nat. Rev. Cancer* **2014**, *14*, 623.

[93] A. Bardelli, K. Pantel, *Cancer Cell* **2017**, *31*, 172.

[94] E. Buscail, C. Maulat, F. Muscari, L. Chiche, P. Cordelier, S. Dabernat, C. Alix-Panabières, L. Buscail, *Cancers* **2019**, *11*, 852.

[95] J.-Y. Douillard, G. Ostoros, M. Cobo, T. Ciuleanu, R. McCormack, A. Webster, T. Milenkova, *Br. J. Cancer* **2014**, *110*, 55.

[96] QIAGEN. therascreen® EGFR RGQ PCR kit instructions for use (handbook), https://www.accessdata.fda.gov/cdrh_docs/pdf12/P120022c.pdf (accessed: May 2020).

[97] F.-C. Bidard, W. Jacot, S. Dureau, E. Brain, T. Bachelot, H. Bourgeois, A. Goncalves, S. Ladoire, H. Naman, F. Dalenc, J. Gligorov, M. Espie, C. Levy, J.-M. Ferrero, D. Loirat, P. Cottu, V. Dieras, C. Simondi, F. Berger, C. Alix-Panabieres, J.-Y. Pierga, *Cancer Research*, American Association for Cancer Research, USA **2019**, pp. GS3-07.

[98] European Liquid Biopsy Society (ELBS), https://www.uke.de/english/departments-institutes/institutes/tumor-biology/european-liquid-biopsy-society-elbs/index.html (accessed: May 2020).

[99] C. Halin, J. R. Mora, C. Sumen, U. H. von Andrian, *Annu. Rev. Cell Dev. Biol.* **2005**, *21*, 581.
[100] T. R. Mempel, S. E. Henrickson, U. H. Von Andrian, *Nature* **2004**, *427*, 154.
[101] S. E. Henrickson, T. R. Mempel, I. B. Mazo, B. Liu, M. N. Artyomov, H. Zheng, A. Peixoto, M. Flynn, B. Senman, T. Junt, H. C. Wong, A. K. .Chakraborty, U. H. von Andrian, *Sci. Signaling* **2008**, *1*, pt2.
[102] M. C. Hunter, A. Teijeira, R. Montecchi, E. Russo, P. Runge, F. Kiefer, C. Halin, *Front. Immunol.* **2019**, *10*, 520.
[103] C. Christodoulou, J. A. Spencer, S.-C. A. Yeh, R. Turcotte, K. D. Kokkaliaris, R. Panero, A. Ramos, G. Guo, N. Seyedhassantehrani, T. V. Esipova, S. A. Vinogradov, S. Rudzinskas, Y. Zhang, A. S. Perkins, S. H. Orkin, R. A. Calogero, T. Schroeder, C. P. Lin, F. D. Camargo, *Nature* **2020**, *578*, 278.
[104] Y. Park, C. A. Best, K. Badizadegan, R. R. Dasari, M. S. Feld, T. Kuriabova, M. L. Henle, A. J. Levine, G. Popescu, *Proc. Natl. Acad. Sci. USA* **2010**, *107*, 6731.
[105] M. Mir, B. Bhaduri, R. Wang, R. Y. Zhu, G. Popescu, *Prog. Opt.* **2012**, *57*, 133.
[106] A. Descloux, K. S. Grußmayer, E. Bostan, T. Lukes, A. Bouwens, A. Sharipov, S. Geissbuehler, A.-L. Mahul-Mellier, H. A. Lashuel, M. Leutenegger, T. Lasser, *Nat. Photonics* **2018**, *12*, 165.
[107] K. Goda, K. K. Tsia, B. Jalali, *Nature* **2009**, *458*, 1145.
[108] K. C. M. Lee, A. K. S. Lau, A. H. L. Tang, M. Wang, A. T. Y. Mok, B. M. F. C., W. Yan, H. C. Shum, K. S. E. Cheah, G. C. F. Chan, H. K. H. So, K. K. Y. Wong, K. K. Tsia, *J. Biophotonics* **2019**, *12*, e201800479.
[109] R. M. Dickson, D. J. Norris, Y. L. Tzeng, W. E. Moerner, *Science* **1996**, *274*, 966.
[110] R. M. Dickson, A. B. Cubitt, R. Y. Tsien, W. E. Moerner, *Nature* **1997**, *388*, 355.
[111] T. A. Klar, S. Jakobs, M. Dyba, A. Egner, S. W. Hell, *Proc. Natl. Acad. Sci. USA* **2000**, *97*, 8206.
[112] T. D. Lacoste, X. Michalet, F. Pinaud, D. S. Chemla, A. P. Alivisatos, S. Weiss, *Proc. Natl. Acad. Sci. USA* **2000**, *97*, 9461.
[113] M. Sauer, M. Heilemann, *Chem. Rev.* **2017**, *117*, 7478.
[114] E. Betzig, G. H. Patterson, R. Sougrat, O. W. Lindwasser, S. Olenych, J. S. Bonifacino, M. W. Davidson, J. Lippincott-Schwartz, H. F. Hess, *Science* **2006**, *313*, 1642.
[115] M. Bates, B. Huang, G. T. Dempsey, X. W. Zhuang, *Science* **2007**, *317*, 1749.
[116] T. Dertinger, R. Colyer, G. Iyer, S. Weiss, J. Enderlein, *Proc. Natl. Acad. Sci. USA* **2009**, *106*, 22287.
[117] M. G. L. Gustafsson, L. Shao, P. M. Carlton, C. J. R. Wang, I. N. Golubovskaya, W. Z. Cande, D. A. Agard, J. W. Sedat, *Biophys. J.* **2008**, *94*, 4957.
[118] L. Schermelleh, P. M. Carlton, S. Haase, L. Shao, L. Winoto, P. Kner, B. Burke, M. C. Cardoso, D. A. Agard, M. G. L. Gustafsson, H. Leonhardt, J. W. Sedat, *Science* **2008**, *320*, 1332.
[119] R. Heintzmann, T. Huser, *Chem. Rev.* **2017**, *117*, 13890.
[120] T. A. Planchon, L. Gao, D. E. Milkie, M. W. Davidson, J. A. Galbraith, C. G. Galbraith, E. Betzig, *Nat. Methods* **2011**, *8*, 417.
[121] B.-C. Chen, W. R. Legant, K. Wang, L. Shao, D. E. Milkie, M. W. Davidson, C. Janetopoulos, X. S. Wu, J. A. Hammer, Z. Liu, B. P. English, Y. Mimori-Kiyosue, D. P. Romero, A. T. Ritter, J. Lippincott-Schwartz, L. Fritz-Laylin, R. D. Mullins, D. M. Mitchell, J. N. Bembenek, A.-C. Reymann, R. Böhme, S. W. Grill, J. T. Wang, G. Seydoux, U. S. Tulu, D. P. Kiehart, E. Betzig, *Science* **2014**, *346*, 1257998.
[122] W. R. Legant, L. Shao, J. B. Grimm, T. A. Brown, D. E. Milkie, B. B. Avants, L. D. Lavis, E. Betzig, *Nat. Methods* **2016**, *13*, 359.
[123] Z. Nizamudeen, R. Markus, R. Lodge, C. Parmenter, M. Platt, L. Chakrabarti, V. Sottile, *Biochim. Biophys. Acta, Mol. Cell Res.* **2018**, *1865*, 1891.
[124] C. Chen, S. Zong, Z. Wang, J. Lu, D. Zhu, Y. Zhang, Y. Cui, *ACS Appl. Mater. Interfaces* **2016**, *8*, 25825.
[125] Y. Xi, D. Wang, T. Wang, L. Huang, X.-E. Zhang, *Nanoscale* **2019**, *11*, 1737.
[126] T. Nerreter, S. Letschert, R. Götz, S. Doose, S. Danhof, H. Einsele, M. Sauer, M. Hudecek, *Nat. Commun.* **2019**, *10*, 3137.
[127] T. S. Barwal, U. Sharma, K. M. Vasquez, H. Prakash, A. Jain, *Biochimie* **2020**, *176*, 62.
[128] C. M. Garcia, S. A. Toms, *World Neurosurg.* **2020**, *138*, 425.
[129] Y. Qi, X. Lu, Q. Feng, W. Fan, C. Liu, Z. Li, *ACS Sens.* **2018**, *3*, 2667.
[130] M. Filius, T. J. Cui, A. N. Ananth, M. W. Docter, J. W. Hegge, J. van der Oost, C. Joo, *Nano Lett.* **2020**, *20*, 2264.
[131] J. Chojnacki, T. Staudt, B. Glass, P. Bingen, J. Engelhardt, M. Anders, J. Schneider, B. Müller, S. W. Hell, H.-G. Kräusslich, *Science* **2012**, *338*, 524.
[132] J. Hanne, F. Göttfert, J. Schimer, M. Anders-Össwein, J. Konvalinka, J. Engelhardt, B. Müller, S. W. Hell, H.-G. Kräusslich, *ACS Nano* **2016**, *10*, 8215.
[133] M. Fritzsche, D. Li, H. Colin-York, V. T. Chang, E. Moeendarbary, J. H. Felce, E. Sezgin, G. Charras, E. Betzig, C. Eggeling, *Nat. Commun.* **2017**, *8*, 14347.
[134] H. Colin-York, Y. Javanmardi, M. Skamrahl, S. Kumari, V. T. Chang, S. Khuon, A. Taylor, T.-L. Chew, E. Betzig, E. Moeendarbary, V. Cerundolo, C. Eggeling, M. Fritzsche, *Cell Rep.* **2019**, *26*, 3369.
[135] T. Lukeš, D. Glatzová, Z. Kvíčalová, F. Levet, A. Benda, S. Letschert, M. Sauer, T. Brdička, T. Lasser, M. Cebecauer, *Nat. Commun.* **2017**, *8*, 1731.
[136] A. M. Santos, A. Ponjavic, M. Fritzsche, R. A. Fernandes, J. B. de la Serna, M. J. Wilcock, F. Schneider, I. Urbančič, J. McColl, C. Anzilotti, K. A. Ganzinger, M. Aßmann, D. Depoil, R. J. Cornall, M. L. Dustin, D. Klenerman, S. J. Davis, C. Eggeling, S. F. Lee, *Nat. Immunol.* **2018**, *19*, 203.
[137] R. Diekmann, D. L. Wolfson, C. Spahn, M. Heilemann, M. Schüttpelz, T. Huser, *Nat. Commun.* **2016**, *7*, 13711.
[138] R. Diekmann, Ø. I. Helle, C. I. Øie, P. McCourt, T. R. Huser, M. Schüttpelz, B. S. Ahluwalia, *Nat. Photonics* **2017**, *11*, 322.
[139] E. Cai, K. Marchuk, P. Beemiller, C. Beppler, M. G. Rubashkin, V. M. Weaver, A. Gérard, T.-L. Liu, B.-C. Chen, E. Betzig, F. Bartumeus, M. F. Krummel, *Science* **2017**, *356*, eaal3118.
[140] F. Balzarotti, Y. Eilers, K. C. Gwosch, A. H. Gynnå, V. Westphal, F. D. Stefani, J. Elf, S. W. Hell, *Science* **2017**, *355*, 606.
[141] L. Gu, Y. Li, S. Zhang, Y. Xue, W. Li, D. Li, T. Xu, W. Ji, *Nat. Methods* **2019**, *16*, 1114.
[142] P. Jouchet, C. Cabriel, N. Bourg, M. Bardou, C. Poüs, E. Fort, S. Lévêque-Fort, *bioRxiv* **2019**, http://biorxiv.org/lookup/doi/10.1101/865865
[143] L. Reymond, J. Ziegler, C. Knapp, F.-C. Wang, T. Huser, V. Ruprecht, S. Wieser, *Opt. Express* **2019**, *27*, 24578.
[144] J. Cnossen, T. Hinsdale, R. Ø. Thorsen, M. Siemons, F. Schueder, R. Jungmann, C. S. Smith, B. Rieger, S. Stallinga, *Nat. Methods* **2020**, *17*, 59.
[145] K. C. Gwosch, J. K. Pape, F. Balzarotti, P. Hoess, J. Ellenberg, J. Ries, S. W. Hell, *Nat. Methods* **2020**, *17*, 217.
[146] A. E. S. Barentine, Y. Lin, M. Liu, P. Kidd, L. Balduf, M. R. Grace, S. Wang, J. Bewersdorf, D. Baddeley, *bioRxiv* **2019**, 606954, http://biorxiv.org/lookup/doi/10.1101/606954
[147] R. B. M. Schasfoort, in: *Handbook of Surface Plasmon Resonance*, (Ed: R. B. M. Schasfoort, Royal Society of Chemistry, Cambridge, UK **2017**, Ch. 1.
[148] J. Homola, J. Dostálek, *Surface Plasmon Resonance Based Sensors*, Springer, Berlin, Germany **2006**.
[149] J. Homola, S. S. Yee, G. Gauglitz, *Sens. Actuators, B* **1999**, *54*, 3.
[150] R. T. Hill, *Wiley Interdiscip. Rev.: Nanomed. Nanobiotechnol.* **2015**, *7*, 152.
[151] S. Scarano, M. Mascini, A. P. F. Turner, M. Minunni, *Biosens. Bioelectron.* **2010**, *25*, 957.

[152] V. Kodoyianni, *BioTechniques* **2011**, *50*, 32.
[153] I. D. Campbell, *Biophysical Techniques*, Oxford University Press, Oxford, UK **2012**.
[154] D. L. M. Rupert, C. Lässer, M. Eldh, S. Block, V. P. Zhdanov, J. O. Lotvall, M. Bally, F. Höök, *Anal. Chem.* **2014**, *86*, 5929.
[155] D. L. M. Rupert, G. V. Shelke, G. Emilsson, V. Claudio, S. Block, C. Lässer, A. Dahlin, J. O. Lötvall, M. Bally, V. P. Zhdanov, F. Höök, *Anal. Chem.* **2016**, *88*, 9980.
[156] A. A. I. Sina, R. Vaidyanathan, S. Dey, L. G. Carrascosa, M. J. A. Shiddiky, M. Trau, *Sci. Rep.* **2016**, *6*, 30460.
[157] A. A. I. Sina, R. Vaidyanathan, A. Wuethrich, L. G. Carrascosa, M. Trau, *Anal. Bioanal. Chem.* **2019**, *411*, 1311.
[158] A. T. Reiner, N.-G. Ferrer, P. Venugopalan, R. C. Lai, S. K. Lim, J. Dostálek, *Analyst* **2017**, *142*, 3913.
[159] Q. Wang, L. Zou, X. Yang, X. Liu, W. Nie, Y. Zheng, Q. Cheng, K. Wang, *Biosens. Bioelectron.* **2019**, *135*, 129.
[160] L. Zhu, K. Wang, J. Cui, H. Liu, X. Bu, H. Ma, W. Wang, H. Gong, C. Lausted, L. Hood, G. Yang, Z. Hu, *Anal. Chem.* **2014**, *86*, 8857.
[161] Y. Fan, X. Duan, M. Zhao, X. Wei, J. Wu, W. Chen, P. Liu, W. Cheng, Q. Cheng, S. Ding, *Biosens. Bioelectron.* **2020**, *154*, 112066.
[162] S. Fang, H. J. Lee, A. W. Wark, R. M. Corn, *J. Am. Chem. Soc.* **2006**, *128*, 14044.
[163] Q. Wang, R. Liu, X. Yang, K. Wang, J. Zhu, L. He, Q. Li, *Sens. Actuators, B* **2016**, *223*, 613.
[164] X. Li, Y. Wang, L. Wang, Q. Wei, *Chem. Commun.* **2014**, *50*, 5049.
[165] H. Šípová, S. Zhang, A. M. Dudley, D. Galas, K. Wang, J. Homola, *Anal. Chem.* **2010**, *82*, 10110.
[166] T. Xue, W. Liang, Y. Li, Y. Sun, Y. Xiang, Y. Zhang, Z. Dai, Y. Duo, L. Wu, K. Qi, B. N. Shivananju, L. Zhang, X. Cui, H. Zhang, Q. Bao, *Nat. Commun.* **2019**, *10*, 28.
[167] Y. Li, A. W. Wark, H. J. Lee, R. M. Corn, *Anal. Chem.* **2006**, *78*, 3158.
[168] L. G. Carrascosa, A. A. I. Sina, R. Palanisamy, B. Sepulveda, M. A. Otte, S. Rauf, M. J. A. Shiddiky, M. Trau, *Chem. Commun.* **2014**, *50*, 3585.7.
[169] U. Eletxigerra, J. Martinez-Perdiguero, R. Barderas, J. M. Pingarrón, S. Campuzano, S. Merino, *Anal. Chim. Acta* **2016**, *905*, 156.
[170] H. Im, H. Shao, Y. I. Park, V. M. Peterson, C. M. Castro, R. Weissleder, H. Lee, *Nat. Biotechnol.* **2014**, *32*, 490.
[171] J. Park, H. Im, S. Hong, C. M. Castro, R. Weissleder, H. Lee, *ACS Photonics* **2018**, *5*, 487.
[172] K. S. Yang, H. Im, S. Hong, I. Pergolini, A. F. Del Castillo, R. Wang, S. Clardy, C.-H. Huang, C. Pille, S. Ferrone, R. Yang, C. M. Castro, H. Lee, C. F. Del Castillo, R. Weissleder, *Sci. Transl. Med.* **2017**, *9*, eaal3226.
[173] S. Zhu, H. Li, M. Yang, S. W. Pang, *Nanoscale* **2018**, *10*, 19927.
[174] D. Raghu, J. A. Christodoulides, M. Christophersen, J. L. Liu, G. P. Anderson, M. Robitaille, J. M. Byers, M. P. Raphael, *PLoS One* **2018**, *13*, e0202773.
[175] A. Finotti, M. Allegretti, J. Gasparello, P. Giacomini, D. Spandidos, G. Spoto, R. Gambari, *Int. J. Oncol.* **2018**, *53*, 1395.
[176] Y.-S. Borghei, M. Hosseini, *Sci. Rep.* **2019**, *9*, 5453.
[177] J. Ki, H. young Lee, H. Y. Son, Y.-M. Huh, S. Haam, *ACS Appl. Mater. Interfaces* **2019**, *11*, 18923.
[178] S. Wei, G. Chen, X. Jia, X. Mao, T. Chen, D. Mao, W. Zhang, W. Xiong, *Anal. Chim. Acta* **2020**, *1095*, 179.
[179] M. Y. Sha, H. Xu, M. J. Natan, R. Cromer, *J. Am. Chem. Soc.* **2008**, *130*, 17214.
[180] W. Shi, R. J. Paproski, R. Moore, R. Zemp, *J. Biomed. Opt.* **2014**, *19*, 056014.
[181] S. Bhana, E. Chaffin, Y. Wang, S. R. Mishra, X. Huang, *Nanomedicine* **2014**, *9*, 593.
[182] C. Sun, R. Zhang, M. Gao, X. Zhang, *Anal. Bioanal. Chem.* **2015**, *407*, 8883.
[183] Y. Pang, C. Wang, R. Xiao, Z. Sun, *Chemistry* **2018**, *24*, 7060.
[184] P. Zhang, R. Zhang, M. Gao, X. Zhang, *ACS Appl. Mater. Interfaces* **2014**, *6*, 370.
[185] X. Wang, X. Qian, J. J. Beitler, Z. G. Chen, F. R. Khuri, M. M. Lewis, H. J. C. Shin, S. Nie, D. M. Shin, *Cancer Res.* **2011**, *71*, 1526.
[186] X. Wu, L. Luo, S. Yang, X. Ma, Y. Li, C. Dong, Y. Tian, L. Zhang, Z. Shen, A. Wu, *ACS Appl. Mater. Interfaces* **2015**, *7*, 9965.
[187] X. Wu, Y. Xia, Y. Huang, J. Li, H. Ruan, T. Chen, L. Luo, Z. Shen, A. Wu, *ACS Appl. Mater. Interfaces* **2016**, *8*, 19928.
[188] Z. A. Nima, M. Mahmood, Y. Xu, T. Mustafa, F. Watanabe, D. A. Nedosekin, M. A. Juratli, T. Fahmi, E. I. Galanzha, J. P. Nolan, A. G. Basnakian, V. P. Zharov, A. S. Biris, *Sci. Rep.* **2015**, *4*, 4752.
[189] Z. Wang, S. Zong, H. Chen, C. Wang, S. Xu, Y. Cui, *Adv. Healthcare Mater.* **2014**, *3*, 1889.
[190] S. C.-H. Tsao, J. Wang, Y. Wang, A. Behren, J. Cebon, M. Trau, *Nat. Commun.* **2018**, *9*, 1482.
[191] H. Ruan, X. Wu, C. Yang, Z. Li, Y. Xia, T. Xue, Z. Shen, A. Wu, *ACS Biomater. Sci. Eng.* **2018**, *4*, 1073.
[192] T. Xue, S. Wang, G. Ou, Y. Li, H. Ruan, Z. Li, Y. Ma, R. Zou, J. Qiu, Z. Shen, A. Wu, *Anal. Methods* **2019**, *11*, 2918.
[193] S. Zong, L. Wang, C. Chen, J. Lu, D. Zhu, Y. Zhang, Z. Wang, Y. Cui, *Anal. Methods* **2016**, *8*, 5001.
[194] Z. Wang, S. Zong, Y. Wang, N. Li, L. Li, J. Lu, Z. Wang, B. Chen, Y. Cui, *Nanoscale* **2018**, *10*, 9053.
[195] E. A. Kwizera, R. O'Connor, V. Vinduska, M. Williams, E. R. Butch, S. E. Snyder, X. Chen, X. Huang, *Theranostics* **2018**, *8*, 2722.
[196] T.-D. Li, R. Zhang, H. Chen, Z.-P. Huang, X. Ye, H. Wang, A.-M. Deng, J.-L. Kong, *Chem. Sci.* **2018**, *9*, 5372.
[197] W. Zhang, L. Jiang, R. J. Diefenbach, D. H. Campbell, B. J. Walsh, N. H. Packer, Y. Wang, *ACS Sens.* **2020**, *5*, 764.
[198] J. Park, M. Hwang, B. Choi, H. Jeong, J.-H. Jung, H. K. Kim, S. Hong, J.-H. Park, Y. Choi, *Anal. Chem.* **2017**, *89*, 6695.
[199] J. Carmicheal, C. Hayashi, X. Huang, L. Liu, Y. Lu, A. Krasnoslobodtsev, A. Lushnikov, P. G. Kshirsagar, A. Patel, M. Jain, Y. L. Lyubchenko, Y. Lu, S. K. Batra, S. Kaur, *Nanomedicine* **2019**, *16*, 88.
[200] Q. Zhou, J. Zheng, Z. Qing, M. Zheng, J. Yang, S. Yang, L. Ying, R. Yang, *Anal. Chem.* **2016**, *88*, 4759.
[201] J. Zhang, Y. Dong, W. Zhu, D. Xie, Y. Zhao, D. Yang, M. Li, *ACS Appl. Mater. Interfaces* **2019**, *11*, 18145.
[202] J. D. Driskell, A. G. Seto, L. P. Jones, S. Jokela, R. A. Dluhy, Y.-P. Zhao, R. A. Tripp, *Biosens. Bioelectron.* **2008**, *24*, 917.
[203] J. D. Driskell, O. M. Primera-Pedrozo, R. A. Dluhy, Y. Zhao, R. A. Tripp, *Appl. Spectrosc.* **2009**, *63*, 1107.
[204] J. L. Abell, J. M. Garren, J. D. Driskell, R. A. Tripp, Y. Zhao, *J. Am. Chem. Soc.* **2012**, *134*, 12889.
[205] Y. Sun, L. Shi, L. Mi, R. Guo, T. Li, *J. Mater. Chem. B* **2020**, *8*, 5178.
[206] C. Liu, C. Chen, S. Li, H. Dong, W. Dai, T. Xu, Y. Liu, F. Yang, X. Zhang, *Anal. Chem.* **2018**, *90*, 10591.
[207] M. Li, S. K. Cushing, J. Zhang, S. Suri, R. Evans, W. P. Petros, L. F. Gibson, D. Ma, Y. Liu, N. Wu, *ACS Nano* **2013**, *7*, 4967.
[208] J. Su, A. F. Goldberg, B. M. Stoltz, *Light: Sci. Appl.* **2016**, *5*, e16001.
[209] F. Vollmer, S. Arnold, D. Keng, *Proc. Natl. Acad. Sci. USA* **2008**, *105*, 20701.
[210] J. Su, *ACS Photonics* **2015**, *2*, 1241.
[211] M. D. Baaske, M. R. Foreman, F. Vollmer, *Nat. Nanotechnol.* **2014**, *9*, 933.
[212] M. D. Baaske, F. Vollmer, *Nat. Photonics* **2016**, *10*, 733.
[213] D. Altschuh, M. C. Dubs, E. Weiss, G. Zeder-Lutz, M. H. V. van Regenmortel, *Biochemistry* **1992**, *31*, 6298.
[214] T. M. Squires, R. J. Messinger, S. R. Manalis, *Nat. Biotechnol.* **2008**, *26*, 417.
[215] M. S. Luchansky, R. C. Bailey, *Anal. Chem.* **2010**, *82*, 1975.
[216] J. Su, *Sensors* **2017**, *17*, 540.
[217] T. C. Oates, L. W. Burgess, *Appl. Spectrosc.* **2011**, *65*, 1187.

[218] G. Keiser, *Biophotonics: Concepts to Applications*, Springer, Berlin, Germany **2016**.
[219] C. Li, L. Chen, E. McLeod, J. Su, *Photonics Res.* **2019**, *7*, 939.
[220] A. L. Washburn, L. C. Gunn, R. C. Bailey, *Anal. Chem.* **2009**, *81*, 9499.
[221] J. D. Suter, D. J. Howard, H. Shi, C. W. Caldwell, X. Fan, *Biosens. Bioelectron.* **2010**, *26*, 1016.
[222] D. K. Armani, T. J. Kippenberg, S. M. Spillane, K. J. Vahala, *Nature* **2003**, *421*, 925.
[223] L. Chen, C. Li, Y.-M. Liu, J. Su, E. McLeod, *Photonics Res.* **2019**, *7*, 967.
[224] R. J. Patton, M. G. Wood, R. M. Reano, *Opt. Lett.* **2017**, *42*, 4239.
[225] E. Ozgur, K. E. Roberts, E. O. Ozgur, A. N. Gin, J. R. Bankhead, Z. Wang, J. Su, *Anal. Chem.* **2019**, *91*, 11872.
[226] D. H. Wilson, D. W. Hanlon, G. K. Provuncher, L. Chang, L. Song, P. P. Patel, E. P. Ferrell, H. Lepor, A. W. Partin, D. W. Chan, L. J. Sokoll, C. D. Cheli, R. P. Thiel, D. R. Fournier, D. C. Duffy, *Clin. Chem.* **2011**, *57*, 1712.
[227] Z. Andreu, M. Yáñez-Mó, *Front. Immunol.* **2014**, *5*, 442.
[228] J. Su, *ACS Photonics* **2016**, *3*, 718.
[229] S. A. Melo, L. B. Luecke, C. Kahlert, A. F. Fernandez, S. T. Gammon, J. Kaye, V. S. LeBleu, E. A. Mittendorf, J. Weitz, N. Rahbari, C. Reissfelder, C. Pilarsky, M. F. Fraga, D. Piwnica-Worms, R. Kalluri, *Nature* **2015**, *523*, 177.
[230] R. A. Waldron, *Proc. IEE C Monogr.* **1960**, *107*, 272.
[231] T. J. A. Kippenberg, Ph.D. Thesis, California Institute of Technology **2004**.
[232] J. Su, *JoVE* **2015**, *106*, e53180.
[233] A. J. Qavi, J. T. Kindt, M. A. Gleeson, R. C. Bailey, *Anal. Chem.* **2011**, *83*, 5949.
[234] F. Dell'Olio, D. Conteduca, C. Ciminelli, M. N. Armenise, *Opt. Express* **2015**, *23*, 28593.
[235] M. Kulis, M. Esteller, *Advances in Genetics* (Eds: T. Friedmann, J. C. Dunlap, S. F. Goodwin, Elsevier, Amsterdam, The Netherlands **2010**, Ch. 2.
[236] J. T. Gohring, P. S. Dale, X. Fan, *Sens. Actuators, B* **2010**, *146*, 226.
[237] H. Inan, M. Poyraz, F. Inci, M. A. Lifson, M. Baday, B. T. Cunningham, U. Demirci, *Chem. Soc. Rev.* **2017**, *46*, 366.
[238] T. D. Canady, N. Li, L. D. Smith, Y. Lu, M. Kohli, A. M. Smith, B. T. Cunningham, *Proc. Natl. Acad. Sci. USA* **2019**, *116*, 19362.
[239] Y. Wang, W. Yuan, M. Kimber, M. Lu, L. Dong, *ACS Sens.* **2018**, *3*, 1616.
[240] K. E. You, N. Uddin, T. H. Kim, Q. H. Fan, H. J. Yoon, *Sens. Actuators, B* **2018**, *277*, 62.
[241] V. S. Lin, *Science* **1997**, *278*, 840.
[242] W. Z. Song, X. M. Zhang, A. Q. Liu, C. S. Lim, P. H. Yap, H. M. M. Hosseini, *Appl. Phys. Lett.* **2006**, *89*, 203901.
[243] P. Y. Liu, L. K. Chin, W. Ser, H. F. Chen, C.-M. Hsieh, C.-H. Lee, K.-B. Sung, T. C. Ayi, P. H. Yap, B. Liedberg, K. Wang, T. Bourouina, Y. Leprince-Wang, *Lab Chip* **2016**, *16*, 634.
[244] X. Xi, T. Li, Y. Huang, J. Sun, Y. Zhu, Y. Yang, Z. J. Lu, *Noncoding RNAs* **2017**, *3*, 9.
[245] Clinical Laboratory Improvement Amendments (CLIA), https://www.cms.gov/regulations-and-guidance/legislation/clia/downloads/howobtaincertificateofwaiver.pdf (accessed: September 2020).
[246] Official website of the CellSearch® System, https://www.cellsearchctc.com/ (accessed: May 2020).
[247] Official website of the Cobas® EGFR Mutation Test v2, https://diagnostics.roche.com/global/en/products/params/cobas-egfr-mutation-test-v2.html (accessed: May 2020).
[248] H. Lee, J. Gurtowski, S. Yoo, M. Nattestad, S. Marcus, S. Goodwin, W. Richard McCombie, M. C. Schatz, *bioRxiv* **2016**. https://doi.org/10.1101/606954
[249] M. C. Liu, G. R. Oxnard, E. A. Klein, C. Swanton, M. V. Seiden, S. R. Cummings, F. Absalan, G. Alexander, B. Allen, H. Amini, A. M. Aravanis, S. Bagaria, L. Bazargan, J. F. Beausang, J. Berman, C. Betts, A. Blocker, J. Bredno, R. Calef, G. Cann, J. Carter, C. Chang, H. Chawla, X. Chen, T. C. Chien, D. Civello, K. Davydov, V. Demas, M. Desai, Z. Dong, et al., *Ann. Oncol.* **2020**, *31*, 745.
[250] Official website of the Galleri®, https://grail.com/galleri/ (accessed: September 2020).
[251] A. McCarthy, *Chem. Biol.* **2010**, *17*, 675.
[252] Official website of PacBio, https://www.pacb.com/ (accessed: September 2020).
[253] Droplet Digital™ PCR (ddPCR™) Technology, https://www.bio-rad.com/it-it/applications-technologies/droplet-digital-pcr-ddpcr-technology?ID=MDV31M4VY (accessed: May 2020).
[254] L. V. Sequist, S. Nagrath, M. Toner, D. A. Haber, T. J. Lynch, *J. Thorac. Oncol.* **2009**, *4*, 281.
[255] J. Zhou, A. Kulasinghe, A. Bogseth, K. O'Byrne, C. Punyadeera, I. Papautsky, *Microsyst. Nanoeng.* **2019**, *5*, 8.
[256] Y. Song, D. Cheng, L. Zhao, *Microfluidics: Fundamentals, Devices and Applications*, Wiley-VCH, Weinheim, Germany **2018**, Ch. 7.
[257] H. Lee, C. Park, W. Na, K. H. Park, S. Shin, *Npj Precis. Oncol.* **2020**, *4*, 3.
[258] O. Behrmann, M. Hügle, P. Bronsert, B. Herde, J. Heni, M. Schramm, F. T. Hufert, G. A. Urban, G. Dame, *PLoS One* **2019**, *14*, e0226571.
[259] J. C. Contreras-Naranjo, H.-J. Wu, V. M. Ugaz, *Lab Chip* **2017**, *17*, 3558.
[260] F. Fachin, P. Spuhler, J. M. Martel-Foley, J. F. Edd, T. A. Barber, J. Walsh, M. Karabacak, V. Pai, M. Yu, K. Smith, H. Hwang, J. Yang, S. Shah, R. Yarmush, L. V. Sequist, S. L. Stott, S. Maheswaran, D. A. Haber, R. Kapur, M. Toner, *Sci. Rep.* **2017**, *7*, 10936.
[261] S. Nagrath, L. V. Sequist, S. Maheswaran, D. W. Bell, D. Irimia, L. Ulkus, M. R. Smith, E. L. Kwak, S. Digumarthy, A. Muzikansky, P. Ryan, U. J. Balis, R. G. Tompkins, D. A. Haber, M. Toner, *Nature* **2007**, *450*, 1235.
[262] S. L. Stott, C.-H. Hsu, D. I. Tsukrov, M. Yu, D. T. Miyamoto, B. A. Waltman, S. M. Rothenberg, A. M. Shah, M. E. Smas, G. K. Korir, F. P. Floyd, A. J. Gilman, J. B. Lord, D. Winokur, S. Springer, D. Irimia, S. Nagrath, L. V. Sequist, R. J. Lee, K. J. Isselbacher, S. Maheswaran, D. A. Haber, M. Toner, *Proc. Natl. Acad. Sci. USA* **2010**, *107*, 18392.
[263] E. Ozkumur, A. M. Shah, J. C. Ciciliano, B. L. Emmink, D. T. Miyamoto, E. Brachtel, M. Yu, P. -i. Chen, B. Morgan, J. Trautwein, A. Kimura, S. Sengupta, S. L. Stott, N. M. Karabacak, T. A. Barber, J. R. Walsh, K. Smith, P. S. Spuhler, J. P. Sullivan, R. J. Lee, D. T. Ting, X. Luo, A. T. Shaw, A. Bardia, L. V. Sequist, D. N. Louis, S. Maheswaran, R. Kapur, D. A. Haber, M. Toner, *Sci. Transl. Med.* **2013**, *5*, 179ra47.
[264] A. C. Lee, J. Svedlund, E. Darai, Y. Lee, D. Lee, H.-B. Lee, S.-M. Kim, O. Kim, H. J. Bae, A. Choi, S. Lee, Y. Jeong, S. W. Song, Y. Choi, H. Yeom, C. S. Lee, W. Han, D. S. Lee, J.-Y. Jang, N. Madaboosi, M. Nilsson, S. Kwon, *Lab Chip* **2020**, *20*, 912.
[265] I. Rodríguez-Ruiz, T. N. Ackermann, X. Muñoz-Berbel, A. Llobera, *Anal. Chem.* **2016**, *88*, 6630.
[266] H. Etayash, A. R. McGee, K. Kaur, T. Thundat, *Nanoscale* **2016**, *8*, 15137.
[267] S. Jeong, J. Park, D. Pathania, C. M. Castro, R. Weissleder, H. Lee, *ACS Nano* **2016**, *10*, 1802.
[268] K. Boriachek, M. N. Islam, V. Gopalan, A. K. Lam, N. T. Nguyen, M. J. A. Shiddiky, *Analyst* **2017**, *142*, 2211.
[269] B. N. Johnson, R. Mutharasan, *Analyst* **2014**, *139*, 1576.
[270] N. Soda, B. H. A. Rehm, P. Sonar, N.-T. Nguyen, M. J. A. Shiddiky, *J. Mater. Chem. B* **2019**, *7*, 6670.
[271] Z. Gao, Z. Yang, *Anal. Chem.* **2006**, *78*, 1470.
[272] B. S. Munge, T. Stracensky, K. Gamez, D. DiBiase, J. F. Rusling, *Electroanalysis* **2016**, *28*, 2644.

Francesco Dell'Olio was awarded his M.Eng. in electronic engineering and Ph.D. in information and communication technologies in 2005 and 2010 from the Polytechnic University of Bari, Italy. Since 2019, he has been an assistant professor of electronics at the same University. In January 2015, he obtained the National Scientific Qualification for the position of the associate professor in electronics. The research interests of Prof. Dell'Olio include the fields of electronics, optoelectronics, and photonics, and he is currently focused on inertial sensors and label-free biosensors.

Judith Su is an assistant professor of biomedical engineering and an assistant professor of optical sciences at the University of Arizona. She received her B.S. and M.S. from MIT in mechanical engineering and her Ph.D. from Caltech in biochemistry and molecular biophysics. Her background is in imaging, microfabrication, and optical instrument building for biological and medical applications.

Thomas Huser is a professor of physics in the Department of Physics at the University of Bielefeld, Germany. His research interests are ultrasensitive optical microscopy and spectroscopy at the level of single cells and single molecules.

Virginie Sottile is an associate professor specialized in stem cell biology and differentiation. Her main research interests center on the regulation of progenitor cell fate choice toward mesenchymal and neural lineages, in healthy tissues and in pathological models such as cancer cells. Her group has also been actively developing interdisciplinary approaches supporting the application of stem cells to tissue repair, initiated at the University of Nottingham (UK) and now proceeding at the University of Pavia (Italy), where she recently joined the Department of Molecular Medicine.

Luis Enrique Cortés-Hernández is a medical doctor from the Autonomous University of Nuevo Leon in Mexico. He then obtained a Masters in comparative vertebrate morphology at Antwerp University, Belgium. Currently, he is a Ph.D. student at Montpellier University, France, and works in the Laboratory of Rare Human Circulating Cells under the supervision of Dr. Catherine Alix-Panabières.

Catherine Alix-Panabières received her Ph.D. degree in Strasbourg (1998). She is an associate professor–director of the Laboratory of Rare Human Circulating Cells at the UMC Montpellier. These last 20 years, she put huge efforts on the analysis of circulating tumor cells in cancer patients.